J Neurophysiol 115: 2105–000, 2016.
First published February 24, 2016; doi:10.1152/jn.00634.2015.

CALL FOR PAPERS | *Neurophysiology of Tactile Perception: A Tribute to Steven Hsiao*

Chronic recordings reveal tactile stimuli can suppress spontaneous activity of neurons in somatosensory cortex of awake and anesthetized primates

Hui-Xin Qi,[1]* Jamie L. Reed,[1]* Joao G. Franca,[1,2] Neeraj Jain,[1] Yoshinao Kajikawa,[1] and Jon H. Kaas[1]

[1]*Department of Psychology, Vanderbilt University, Nashville, Tennessee; and* [2]*Institute of Biophysics Carlos Chagas Filho, Federal University of Rio de Janeiro, Rio de Janeiro, Rio de Janeiro, Brazil*

Submitted 25 June 2015; accepted in final form 19 February 2016

Qi HX, Reed JL, Franca JG, Jain N, Kajikawa Y, Kaas JH. Chronic recordings reveal tactile stimuli can suppress spontaneous activity of neurons in somatosensory cortex of awake and anesthetized primates. *J Neurophysiol* 115: 2105–000, 2016. First published February 24, 2016; doi:10.1152/jn.00634.2015.—In somatosensory cortex, tactile stimulation within the neuronal receptive field (RF) typically evokes a transient excitatory response with or without postexcitatory inhibition. Here, we describe neuronal responses in which stimulation on the hand is followed by suppression of the ongoing discharge. With the use of 16-channel microelectrode arrays implanted in the hand representation of primary somatosensory cortex of New World monkeys and prosimian galagos, we recorded neuronal responses from single units and neuron clusters. In 66% of our sample, neuron activity tended to display suppression of firing when regions of skin outside of the excitatory RF were stimulated. In a small proportion of neurons, single-site indentations suppressed firing without initial increases in response to any of the tested sites on the hand. Latencies of suppressive responses to skin indentation (usually 12–34 ms) were similar to excitatory response latencies. The duration of inhibition varied across neurons. Although most observations were from anesthetized animals, we also found similar neuron response properties in one awake galago. Notably, suppression of ongoing neuronal activity did not require conditioning stimuli or multi-site stimulation. The suppressive effects were generally seen following single-site skin indentations outside of the neuron's minimal RF and typically on different digits and palm pads, which have not often been studied in this context. Overall, the characteristics of widespread suppressive or inhibitory response properties with and without initial facilitative or excitatory responses add to the growing evidence that neurons in primary somatosensory cortex provide essential processing for integrating sensory stimulation from across the hand.

inhibitory period; latency; area 3b; area 3a; monkeys

AMONG THEIR COMMON TRAITS, primates, to varying degrees, rely on remarkable sensory and motor functions of the hand and arm. The cortical representations of the hand and associated neuron properties have long been studied to understand normal and impaired processing of somatosensory stimuli, with emphasis on developing strategies to promote recovery when processing is impaired. Examinations of widespread and multidigit interactions in area 3b have added to our understanding of early stages of somatosensory processing to incorporate neurons with larger response fields that show reductions as well as increases in firing rate when discrete regions of skin are touched (DiCarlo et al. 1998; Fitzgerald et al. 2006b; Friedman et al. 2008; Kim et al. 2015; Reed et al. 2008, 2011; Thakur et al. 2006, 2012). Still, little information is available about the inhibitory components of the receptive field (RF) of neurons related to the hand and arm in primary somatosensory cortex in primates.

Here, we studied characteristics of response suppression in primate primary somatosensory cortex when the hand is touched, and we consider how the response patterns correlate with inhibitory processes in neural circuits across the hand representation. As quoted by Hsiao and colleagues in Thakur et al. (2012): "Previous studies in area 3b have revealed overlapping excitatory and inhibitory inputs throughout the RF of the neuron (Alloway and Burton 1991; Dykes et al. 1984). However, infield inhibition is rarely revealed by single punctate probes (Iwamura et al. 1983; Mountcastle and Powell 1959; Sur 1980; Sur et al. 1984), which show area 3b RFs as homogeneous excitatory regions (Sur 1980)." The term "infield inhibition" refers to the inhibitory field that spatially overlaps the excitatory response and can have some delay or duration that extends beyond excitatory transient responses (Gardner and Costanzo 1980a, b).

The main goal of the present study was to characterize firing suppression in response to tactile stimulation of a single location inside or outside of the minimum (threshold) excitatory RF in somatosensory cortex areas 3b and 3a of anesthetized and awake primates. The studies were conducted using chronically implanted electrode arrays (2×8) in galagos, squirrel monkeys, and one owl monkey, where the primary somatosensory cortical hand representation is exposed on the surface of the brain. We examined cortical neurons in area 3b of primates to explore the nature of information processing in primary somatosensory cortex with emphasis on how stimuli outside of the excitatory RF modulate neuronal activity. Previously, we have reported (Reed et al. 2010a, b, 2011) that area 3b neurons are modulated by stimuli presented outside of the minimal RFs

* H.-X. Qi and J. L. Reed contributed equally to this work.

Address for reprint requests and other correspondence: J. H. Kaas, Dept. of Psychology, Vanderbilt Univ., 301 Wilson Hall, 111 21st Ave. South, Nashville, TN 37240 (e-mail: jon.h.kaas@vanderbilt.edu).

(mRFs), such that stimulation on two different digit or palm sites can facilitate or suppress firing relative to single-site stimulation within the mRF. With the use of chronic microelectrode array recordings, here, we report suppression of baseline firing in response to single-site skin indentations and describe properties of responses related to types of suppression encountered in three different primate species. These latencies of suppression were relatively short and not statistically distinguishable from response facilitation latencies.

With the use of microelectrode arrays with known spacing between electrodes, we were able to identify firing suppression in response to single-site stimulation and determine somatotopic organization for a portion of primary somatosensory cortex. We found that passive single-site stimulation with skin indentations on the hand could evoke different response types (suppression of firing alone as well as excitation followed by suppression) in three different species and generally across awake and anesthetized conditions. We examined the latencies and durations of response suppressions with respect to stimulus location on the hand to detect relationships relevant to the somatotopic organization of cortex. Individual neurons responded to single-site stimulation at different hand locations with different response profiles that could include excitation ("E"), inhibition ("I"), or no response, depending on the location of the stimulus across the surface of the hand. The results further indicate that widespread spatial integration of information originating across different parts of the hand occurs as early as in areas 3b and 3a. Our evidence for long-range interactions between neurons within the hand representations of somatosensory cortex suggests that these neurons are involved in processing information from receptors across large portions of the hand, thus providing an early and necessary step toward the integration of somatosensory information that leads to object perception (Hsiao 2008; Hsiao and Bensmaia 2008; Saal and Bensmaia 2014).

MATERIALS AND METHODS

Experiments were conducted on two prosimian galagos (*Otolemur garnettii*), two squirrel monkeys (*Saimiri sciureus*), and one owl monkey (*Aotus trivirgatus*). These animals were adult males. All procedures involving animals followed the U.S. National Institutes of Health *Guide for the Care and Use of Laboratory Animals* and were approved by the Vanderbilt University Institutional Animal Care and Use Committee.

To record chronically from somatosensory cortex, arrays of 16 electrodes were implanted in the hand representation of area 3b of one or both cerebral hemispheres in each animal. The electrode arrays consisted of Teflon-coated stainless-steel or tungsten microwires, 35 or 50 μm in diameter, spaced 0.25 mm apart in a 2×8 array. Each array was 2 mm long and 0.4 mm wide (Jain et al. 2001; Nicolelis et al. 1998, 2003).

Surgical Procedures

To implant the electrode arrays, each animal was anesthetized with ketamine hydrochloride (25 mg/kg im) and xylazine (0.4 mg/kg im). Supplemental injections were given as needed to maintain a surgical level of anesthesia. Dexamethasone was given (2 mg/kg im) to prevent or reduce brain swelling. Fluids were given subcutaneously, body temperature was maintained with a water-circulating heating pad, and heart rate and respiration were monitored. Two to four stainless screws were placed in the skull for securing ground wires, and two titanium bone screws were placed in the skull to stabilize the array. A small craniotomy was made over the part of area 3b that represents the hand in one or both cerebral hemispheres, and the dura was retracted. To guide the placement of the electrode array, a single microelectrode (1 MΩ impedance at 1 kHz) was used to record multi-unit (MU) activity evoked by light touch on the body and to identify the rostral and caudal borders of the hand representation in area 3b. Once the locations of interest were established, isoflurane (1.5% in 100% oxygen) gas was used for anesthesia. The microelectrode array was oriented so that all of the wires contacted the cortical surface before it was lowered either manually or with a burst-advancing motion by a microdrive (David Kopf Instruments, Tujunga, CA) to a depth of 700-1,000 μm below the pia surface, corresponding approximately to layers III–V. The arrays were secured to the skull with super glue and dental cement. The skin opening was closed with sutures. The animal was treated with antibiotics, carefully monitored, and returned to its home cage after fully recovering from anesthesia.

Data Acquisition

In each recording session, neuronal responses to hand stimulation were collected in animals that were lightly anesthetized with ketamine (10 mg/kg) to reduce any tendency for hand movements. Supplemental injections were given to maintain a light level of anesthesia as needed. The hand was pressed into a clay surface mold to keep it stable. One galago (PG-A) became so habituated to the procedures that stimulation was possible during the fully awake condition.

A multi-electrode array workstation (MEA; Plexon, Dallas, TX) was used to collect waveforms and timestamps with 40 kHz sampling (25 μs analog-to-digital conversion) at 12-bit resolution. Neurophysiological data were analyzed using NeuroExplorer (Nex Technologies, Madison, AL) and MATLAB software (MathWorks, Natick, MA). The preamplified analog neural signals were filtered (cut-off level 250 Hz–3 kHz) and amplified through the MEA. We used automatic and manual thresholding, such that the signals for both single units (SUs) and MUs must cross at least two times the SD of the average noise [see Nicolelis et al. (1997, 2003)]. Time-amplitude discrimination and principal component algorithms (PCAs) were used to isolate SU and MU responses in real time, which were also saved for offline sorting. Each neuronal spike was represented by a single data point in a PCA plot. Clusters of neuronal spikes that were clearly separated from the origin of the PCA plot and from other clusters were considered SUs. The identification of SUs was confirmed offline by autocorrelograms or interspike interval histograms using Nex software, as previously described (Jain et al. 2001; Nicolelis and Chapin 1994). Our classification of SUs included clusters of a few waveforms of similar shape, whereas we classified signals as MUs when several clusters of waveforms of differing shapes could not be isolated separately.

Mapping RFs. Ten days after implantation of the electrode arrays and during subsequent recording sessions over the following months, mRFs were determined from all electrodes in the array for SUs and MUs that responded to tactile stimulation. mRFs (Jain et al. 2001; Merzenich et al. 1978; Nelson et al. 1980; Sur et al. 1982) were defined as the skin region, where light contact just above threshold, produced by a fine probe or a small brush, evoked maximal neural activity. The mRFs represent the center of a larger excitatory RF that can be driven by more intense stimuli. The extent of the mRFs was outlined on drawings of the hand and of other relevant skin surfaces. If tactile stimuli were ineffective, then digits and the hand were moved and tapped in an effort to elicit deep receptor and high threshold responses, which were also noted. Along with histological reconstruction, results of mRF mapping were used to aid estimates of the locations of the 16-electrode arrays, as illustrated, in part, by the example from galago PG-B in Fig. 1.

Tactile stimulation. Quantitative data on the responses of single neurons and small clusters of neurons were acquired separately over a series of 4- to 6-h recording sessions that occurred once or twice/

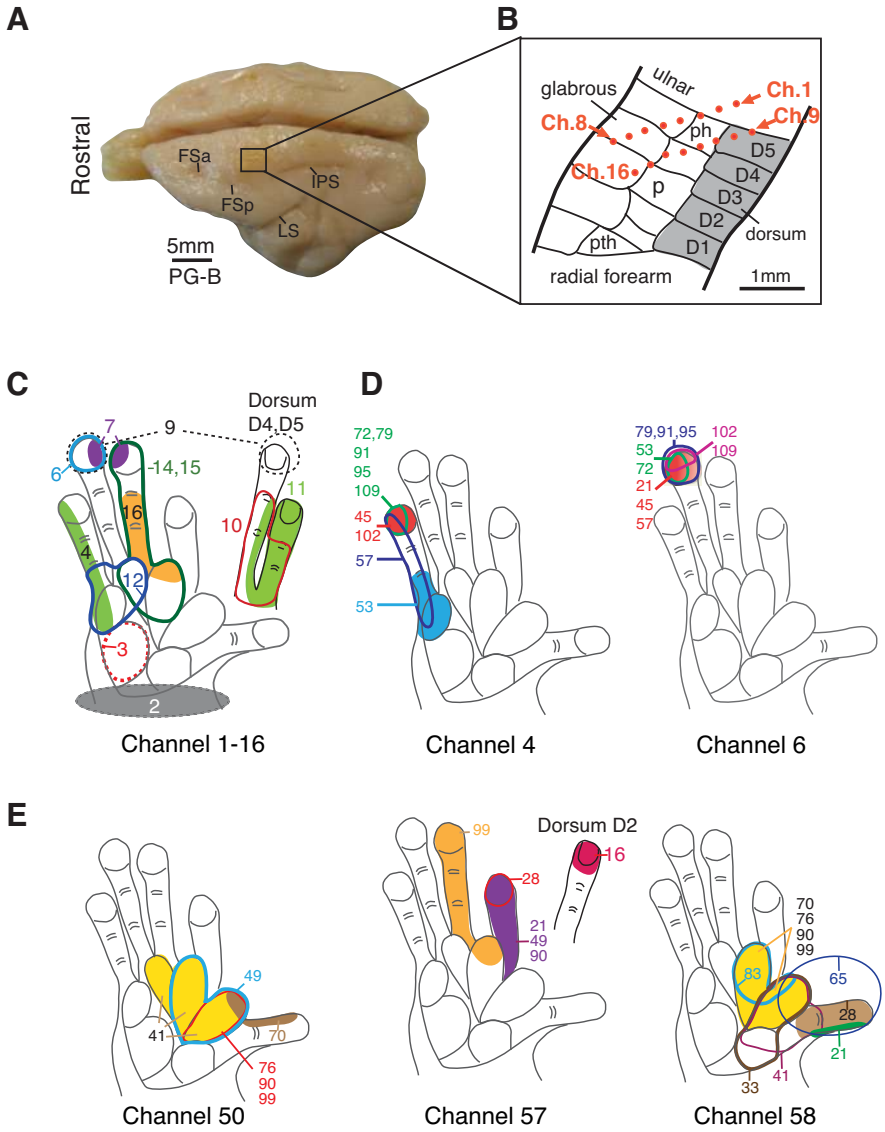

Fig. 1. Example of the location of a multi-electrode array and neuronal receptive fields (RFs) in galago PG-B indicates that RFs can match the expected cortical somatotopy and may change across different recording sessions from the same chronic implant. *A*: photograph of the brain for PG-B shows the location of a multi-electrode array in the left hemisphere of somatosensory cortex. Frontal sulcus anterior (FSa), frontal sulcus posterior (FSp), intraparietal sulcus (IPS), and the lateral sulcus (LS) are indicated as landmarks on the photograph. *B*: schematic drawing shows the approximate microelectrode locations in area 3b of galago PG-B, indicated by orange dots placed on a template based on Wu and Kaas (2003). Positions of the microelectrodes were estimated from tissue reconstructions and from the somatotopy of a hand representation obtained through the array recordings. Ch., channel; D, digit; ph, hypothenar palm pad; P, palm; pth, thenar palm pad. *C*: neuronal RFs from each electrode channel (numbered from 1 to 16) obtained 60 days after array implantation are shown as examples. Note that their locations and sizes, shown in colored shadings and contours, correspond well to the estimated position of the array in cortex. *D*: repeated mapping of RFs (colored shadings and contours) for neurons recorded from channels 4 and 6 show examples of RF changes or stability over time. Numbers indicate days since array implantation when the RFs were mapped. Note that RFs obtained from channel 6 were relatively stable over a period of >3 mo, but RFs obtained from channel 4 shifted during the same period. *E*: examples from area 3a (galago PG-A) of repeated mapping of RFs (colored shadings and contours) for activity recorded from channels 50, 57, and 58 show RF changes over time.

week over a period of many weeks. Cortical neurons were stimulated by punctate square-wave skin indentations generated by a computer-controlled Chubbuck electromechanical stimulating system (Chubbuck 1966). The stimulation probe had a cone shape that tapered to a 1-mm-diameter flat circular tip. For each experiment, the probe was positioned manually over a location of interest on the hand, and the neuronal activity was monitored through an oscilloscope and a speaker, while the probe was lowering to contact the skin. Once responses indicating contact of the skin were detected, a displacement value for the probe was selected (the indentation was usually at 200–500 μm). The Chubbuck probe completely retracted off the skin between pulses without a constant ramp. A constant force (60 g) was applied throughout the indentation on all of the experiments. Repetitive stimuli were delivered for 5 min in each recording stimulation site in the skin. A time and waveform generator (Tucker-Davis Technologies, Alachua, FL) was used to generate a square-wave pulse that controlled the Chubbuck stimulator. Time stamps were simultaneously sent to the multi-electrode array workstation to record the precise times of stimulation. The square-wave pulses produced either 20 ms indentations at 1–30 Hz or 500 ms indentations alternating with 1,500 ms probe retraction. We focused on results obtained with 20 ms skin indentations at low repetition rates (1–2 Hz).

Data Analysis

For each unit, the peri-stimulus time histogram (PSTH) was obtained from all trials per stimulation site. Responses to stimulus onset and stimulus removal were estimated as average firing rates (impulses/second) during two poststimulus time epochs of 10–25 and 25–40 ms using in-house MATLAB scripts. The mean firing rate for onset or offset responses was corrected for the baseline firing rate, corresponding to the activity recorded within a 50-ms period before the stimulus.

To estimate inhibitory response-onset latency, PSTHs were generated using bin sizes that ranged from 1 to 10 ms to optimize temporal resolution, depending on relative response strength and the level of baseline activity. Response latencies were calculated from these PSTHs using a window stepped every 1 ms, regardless of the PSTH bin size. Here, we report the latency and duration of periods of inhibition calculated by setting the threshold at 1.65 times the SD below the mean baseline firing rate, equivalent to a one-tailed significance level of 0.05 for a normal distribution. Only suppression that lasted for 10 ms or longer was classified as inhibition to avoid counting random firing fluctuations as inhibition.

The excitatory peak firing rates and latencies were not the focus of this study. However, the maximum firing-rate magnitude and the time at which the maximum firing occurred were collected from a PSTH

with 1 ms bins and a smoothing filter width of five bins. The maximum firing rate was considered a significant response if the value exceeded the upper 95% confidence limit of the average firing rate. The excitatory response latency was defined as the time at which the firing rate exceeded the mean baseline firing at two times the SD of the baseline ongoing activity.

Firing rates, response latencies, unit classification, and identifying information were compiled in an electronic spreadsheet (Excel; Microsoft, Redmond, WA) and imported into SPSS software (version 22; IBM, Armonk, NY) for summary analyses. Nonparametric tests compared distributions and medians for measures, such as inhibition latency between two categories, with appropriate tests selected for number of comparisons (Kolmogorov-Smirnov test, Mann-Whitney test, median test). For comparing more than two categories, Kruskal-Wallis tests were used with post hoc correction applied for pair-wise comparisons. The nonparametric Spearman's ρ correlation coefficient was used to assess relationships of rank orders between two categories of data. For example, we assessed relationships between measures of inhibition latency and duration with measures of peak firing magnitude. For all tests, unless otherwise indicated, the significance level was set at 0.05 with two-tailed P values.

Note that we follow the convention of referring to firing-rate suppression as "inhibition" and "inhibitory response," even though we are not recording the presence of inhibitory potentials (Sachdev et al. 2012). We also use firing-rate suppression, referred to as I here, as an indicator of the cortical and subcortical processes that may involve inhibition.

Stability of chronic array recordings. The stability of chronic recordings can be evaluated, in part, by examining changes in RF properties (e.g., locations and sizes) over time. We found RFs that were largely stable for some neuron units, which is consistent with some reports [e.g., Jain et al. (2001)], whereas other neuronal RFs in our sample were variable (Fig. 1). For example (Fig. 1*D*), the RFs for neurons recorded from electrode six of galago PG-B remained on distal digit 5 (D5) from day 21 to 109 after array implantation in area 3b. However, in another example recorded from electrode four of the same array, the RFs shifted within D5 over a period of 3–4 mo.

The analysis of waveform shape is the standard way of identifying SUs, but because we characterized the neuronal responses over hours in a single recording session and over multiple days in a series of recording sessions, it is unclear whether the activity of a given unit over time corresponds to recordings from that same neuron over days. To compare neuronal responses (e.g., firing rates and latencies) with tactile stimulation on different locations of the hand, we needed to maintain recordings from the same neurons during all of the recording session within 1 experimental day. We used a technique for array implantations, in which the array is fixed relative to the skull (Jain et al. 2001; Nicolelis et al. 1998, 2003). Since the array was not floating with the brain, normal movements of the brain in the skull could affect the stability of recording over time. During a single recording session, unit waveforms generally appeared quite stable within the same day, irrespective of the number and location of the stimulation sites on the hand (Fig. 2*A*). In this investigation of waveform stability, we exported timestamps containing waveform information recorded in MEA to Excel using NeuroExplorer. For each recording file (usually during stimulation of a single location on the hand for 5 min), we averaged the waveforms of an SU from a given stimulation location and then superimposed all averaged waveforms from different stimulation locations on a line graph. Furthermore, we examined the signals over extended periods comprising multiple experimental sessions. We used the same averaging strategy and displayed all of the mean waveforms from a given unit as a function of time for stimulation at different sites in a single recording session. However, the mean waveforms tend to change gradually over a period of weeks, as shown in the example in Fig. 2*B*. These changes in neuronal recordings, based on characteristics of the extracellular recordings over weeks of time, are consistent with other examinations of the recording stability (Arce-McShane et al. 2014; Dickey et al. 2009).

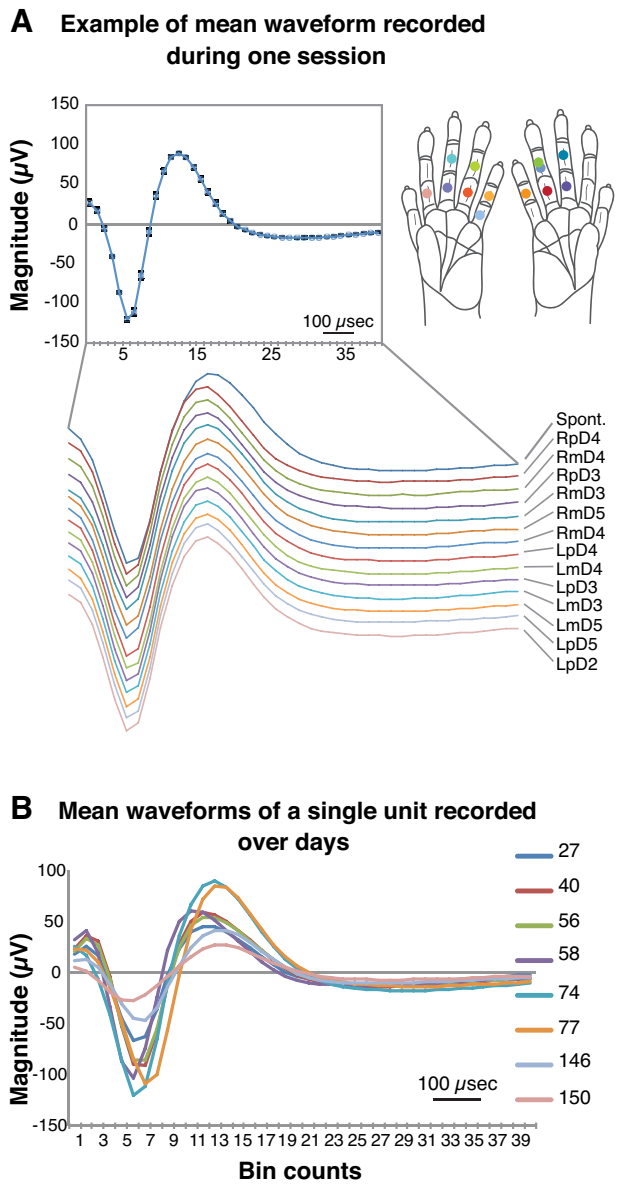

Fig. 2. Stability of mean waveforms recorded with a chronically implanted array in squirrel monkey SM-A. The x-axis of both panels shows 40, 25-μs bins from which the waveforms were sampled (25 μs analog-to-digital conversion rate). *A*: mean waveform of unit 8a recorded during the same session. Line graphs depict mean waveforms of signals recorded from a neuron unit (8a) during tactile stimulation on 13 locations on the hand and during no stimulation [spontaneous (Spont.)] within 1 recording day. Different stimulation conditions are indicated by the text (at the right end of the line) and the colors of the mean waveform lines, as well as matching colored dots on the different stimulation sites on the hand schematics (*inset*, *right*). L, left (hand); m, middle; p, proximal; R, right (hand). For the given recording day (*inset*, *top left*), the mean waveform displaying small SDs for individual data points also indicates a highly stable activity within a single recording day. *B*: mean waveforms collected in channel 8 over different days. Line graphs depict mean waveforms of the same neuron (8a) recorded over 5 mo. The number of days after array implantation is noted next to each colored line in the key. In the figure, overlapping lines and visible differences in amplitude (y-axis magnitude) and duration (x-axis bin counts) indicate the waveform fluctuation over time.

Based on these findings, illustrated in Figs. 1 and 2, we treated an SU from a given electrode throughout each recording day as the same neuron. However, we considered units recorded from a given

Table 1. *Recording information*

Case	Species	Recording Sessions	Unit Occurrence	SUs	MUs
SM-A	Squirrel monkey	5	421	133	288
SM-B	Squirrel monkey	4	217	93	124
PG-A (awake, 3a)	Galago	6	98	51	47
PG-B	Galago	11	369	143	226
OM-A	Owl monkey	6	261	5	256
Total		32	1,366	425	941

SUs, single units; MUs, multi-units.

electrode on different days as different units due to the fluctuations in the unit properties in our samples. This practice could lead to a bias, because the same neuron could be represented multiple times as different unit responses; however, this bias is mitigated by our focus primarily on the ranges of values obtained in measurements for inhibition latency, duration, and spatial relationships within the stimulus presentation area on the hand. Note that the proportions of the occurrences of various response types are affected by this bias and should not be considered to represent populations of neurons.

Histology. To visualize the positions of the electrodes in the electrode arrays in the histologically identified hand region of somatosensory area 3b, brain sections were processed either for cytochrome oxidase (Wong-Riley 1979) or Nissl substance. After the terminal experiment, the animals were given lethal injections (80 mg/kg or more) of pentobarbital. When areflexive, they were perfused through the heart with PBS (pH 7.4), successively followed by 4% paraformaldehyde in phosphate buffer and 4% paraformaldehyde with 10% sucrose in phosphate buffer. The brain was removed, and the thalamus was separated from the cortex. A block of frontoparietal cortex was separated from the rest of cortex, immersed in 30% sucrose in phosphate buffer, and refrigerated until the next day. The block containing the parietal cortex was cut parasagittally across the width of somatosensory cortex on a freezing microtome into 50 μm sections. The penetration depths of the electrodes in the arrays were determined from electrode tracts in the parasagittal brain sections in every other section processed for Nissl substance or cytochrome oxidase.

RESULTS

The results presented here represent a subset of the data of recorded units that displayed suppressive responses. Total recording sessions and unit responses for each case are shown in Table 1. All recordings were obtained from chronically implanted arrays of microelectrodes. A single 16-electrode array was implanted in somatosensory cortex of one New World owl monkey (OM-A) and one prosimian galago (PG-A), whereas an array was implanted in each hemisphere of one galago (PG-B) and two squirrel monkeys (SM-A, SM-B). In four cases, electrodes were in the hand region of area 3b of somatosensory cortex. Electrode tips were in layers IV and V. In one case (PG-A), the electrode array was in area 3a, and the electrode tips were in layers III and IV. The locations of the electrodes were histologically confirmed to be in the hand representation of area 3b or area 3a, as previously determined in microelectrode mapping studies (Carlson and Welt 1980;

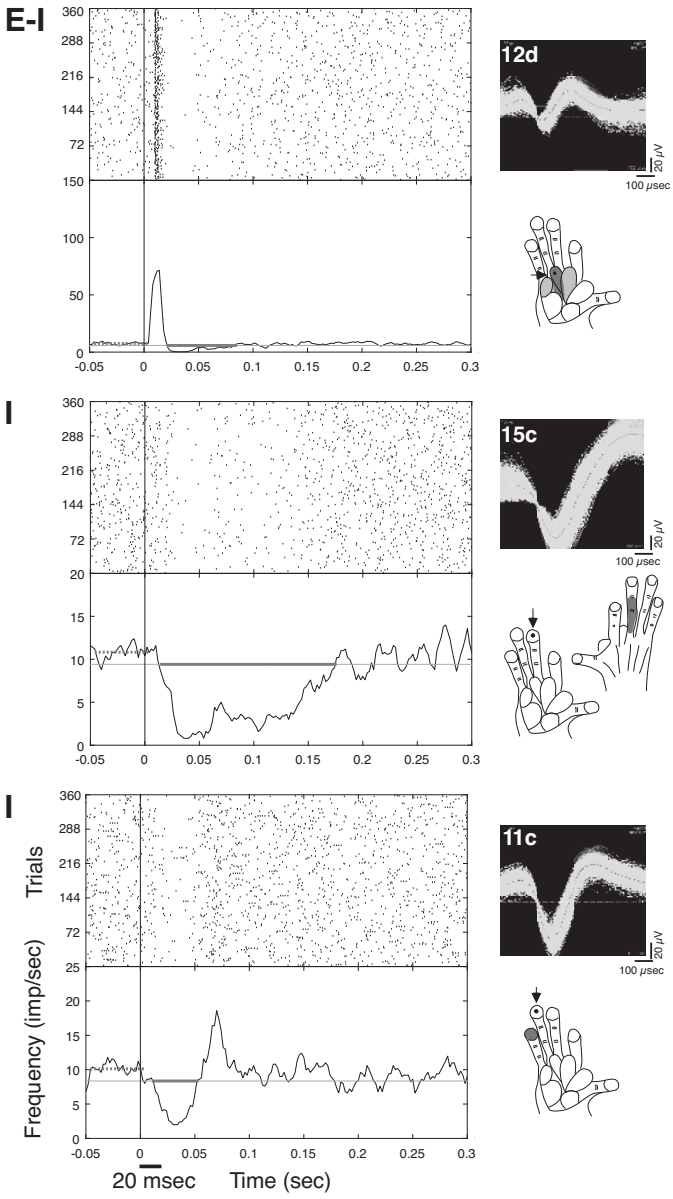

Fig. 3. Peri-stimulus histograms (PSTHs) and rasters show different "response types" to single-site stimulation on the hand for galago PG-B and indicate measures of suppression latency and duration. In all panels, the thick, gray horizontal lines on the PSTHs (*left*) show the period for which the firing was suppressed below baseline, indicating the latency and duration of the suppression for that neuron. Line PSTHs are smoothed with a Gaussian filter (filter width = 5, 1-ms bins). The *y*-axes of the PSTHs are firing frequency [impulses/second (imp/sec)], with trial numbers on the *y*-axes for the rasters (as depicted in the bottom graph). Stimulus repetition rate was 1 Hz with 20 ms indentations on the skin. Stimulus onset and duration are indicated by the black line below the *x*-axis in the bottom graph. Waveforms of the example units are shown to the right of the PSTHs and rasters, along with schematics of the galago hand, indicating stimulus sites (dots and arrows) and mapped RF locations (gray shading). Darker shading indicates stronger excitatory responses to tactile stimulation, whereas lighter shading indicates weaker but detectable excitatory responses. *Top*: excitatory responses followed by postexcitatory suppression for neuron unit 12d in response to single-site stimulation on pad 2 is an example of an excitatory-inhibitory ("E-I") response. *Middle*: in an example of an inhibitory ("I") response, ongoing baseline activity was suppressed in neuron 15c of galago PG-B for relatively long durations during single-site skin indentation on distal D3 (dD3). Note that the mapped RF was on dorsal D3 (*right* schematic), and stimulation on glabrous dD3 suppressed firing (*left* schematic). *Bottom*: in another example of a type I response, ongoing spontaneous activity was suppressed relatively briefly and followed by rebound firing increases for unit 11c. Note that this suppression response occurred when the stimulus site on dD4 was adjacent to the mapped minimal RF (mRF) site on dD5 for the given recording session.

Sur et al. 1980; Wu and Kaas 2003). The locations of the RFs of neurons recorded in the two rows of each electrode array were consistent with the known somatotopy and the sizes of the mRFs of neurons or neuronal clusters determined in previous microelectrode mapping experiments. Thus progressions of mRFs for caudorostral rows of recording sites located in area 3b typically start on the wrist or hairy hand and progress to or near the glabrous fingertips (Fig. 1).

Response Properties of Neurons in Area 3a in an Awake Galago

Unlike area 3b, many neurons in area 3a of anesthetized New World monkeys and prosimian galagos respond poorly to light tactile stimuli, as strong thalamic activation is relayed from muscle spindle receptors and probably other proprioceptive receptors (Huffman and Krubitzer 2001; Merzenich et al. 1983; Wu and Kaas 2003). However, responses to tactile stimuli can be recorded, as area 3b provides an input to area 3a (Krubitzer and Kaas 1990; Wu and Kaas 2003). For example, in lightly anesthetized baboons, a portion of neurons in area 3a was found to respond only to cutaneous stimulation, whereas others respond to both muscle and cutaneous or muscle stimulation alone (Heath et al. 1976). In one galago that was amenable to tactile stimulation in the awake condition and had an array implanted in area 3a (PG-A), we were able to record responses to skin indentations. In this and all other cases included in our study, we did not characterize responsiveness to deep pressure or movement.

In response to tactile stimulation on the hand, area 3a neurons in PG-A displayed response properties similar to those of neurons in area 3b. However, area 3a cutaneous RFs in the awake galago were usually larger than in area 3b. Area 3a neuronal RFs often covered several digits, the entire palm, or even the entire hand (Fig. 1*E*). Results from all cases are discussed together to follow, with exceptions noted when appropriate.

Typical Response Characteristics of Neurons in the Hand Representation of Areas 3b and 3a

In both New World monkeys and prosimian galagos, neurons in area 3b responded to tactile stimuli within the mRF in ways expected from previous descriptions (Jain et al. 2001; Reed et al. 2010b). Area 3a neurons responded to cutaneous stimulation in similar patterns compared with recordings from area 3b in anesthetized primates. Our results refer to response occurrences, for which neural activity recorded within a session was considered to originate from stable SUs and MUs, whereas activity from the same electrode across different days could vary in origin (Figs. 1 and 2). We focused our analysis on types of suppressive response occurrences (Fig. 3), in which neuronal activity was either suppressed by tactile stimulation without an initial firing increase (classified as inhibitory, or I responses) or presented a transient period of excitation, followed by a period of firing suppression (classified as excitatory-inhibitory, "E-I" responses).

With the use of chronically implanted electrodes, we tracked the neural activity recorded in response to tactile stimulation on different locations on the hand. Because we recorded simultaneously from 16 electrodes, we collected considerable amounts of data in which skin indentations were delivered outside regions evoking peak activation. Within the same recording day, most SUs and MUs included in this study were characterized first by identifying the region on the hand where skin indentations evoked the strongest neuronal discharge (peak activation location). After the identification of suppressive response occurrences from a given unit, firing in response to stimulation of the peak activation location and each additional stimulated location was classified as E, E-I, I, or "NS" (for no significant firing change). Note that a given unit could present different neuronal response types depending on the stimulus location on the hand (e.g., Fig. 4).

In our sample, most neurons responded to a brief skin indentation with a transient increase in firing rate, followed by a decrease in firing rate and then a return to baseline level or even below baseline rates (E-I response type). For a suprathreshold skin indentation, a minority of cortical neurons exhibited suppression of baseline activity that was established after the stimulus and then sustained for a short period (I response type) [also, see Sur et al. (1984)]. These responses of neurons in area 3b (S1) of galagos, squirrel monkeys, and owl monkey resemble those reported for other primates [e.g., Jain et al. (2001)] in this regard. The distributions of suppressive response types were the same for neurons in area 3b (anesthetized) and area 3a (unanesthetized galago) across the New World monkeys and galagos (Mann-Whitney U-test $= 9.21 \times 10^4$, $Z = -1.56$, $P = 0.119$, $n = 946$ responses). Additionally, data from area 3a were collected from one case only (PG-A); thus we summarized values from all cases (areas 3a and 3b) for the results. Table 2 reports data from areas 3a and 3b separately. However, a small subset of data was collected from area 3a (PG-A; see Figs. 5*B*, 6*B*, and 7); therefore, statistical analyses are presented in Table 2 for area 3b alone, along with

Fig. 4. A typical response profile in galago PG-B is illustrated by tracking the activity of a given single unit (SU; 11a), in response to stimulation on several hand sites within 1 recording session. *A*: the location of the electrode channel 11 is indicated with a green outline and arrow on the schematic of area 3b from Wu and Kaas (2003) (see Fig. 1). *B*: images from the Offline Sorter software (Plexon) show the recorded waveforms from electrode channel 11, indicating separate isolation of unit 11a (yellow) from other recorded activity on electrode 11 (green). *C*: schematic of the galago hand indicates the hand sites stimulated during the illustrated recording session, with symbols and color shading as visual representations of responses to stimulation. The "+" symbols represent excitatory ("E"; or E-I) responses, with red shading indicating the stimulus site that evoked the highest peak response, termed the "hot spot." Lighter red shading indicates excitatory responses with lower magnitudes than the hot spot. Blue shading and the "−" symbols represent inhibitory (I) responses. The "x" symbol indicates a site that was stimulated, but no significant ("NS") change in firing was detected. For visualization purposes, shaded regions indicate phalanges or palm pads on which the stimulus probe was placed. The shading in the response profile figures may not specifically detail the boundaries of mRFs. In this "complex response profile," a hot spot is flanked by weaker E and E-I, I, and NS regions of no significant response. *D*: rasters and PSTHs show the responses to single-site stimulation on each of the hand locations tested from the recording session shown in *C*. The PSTH and raster plot corresponding to the stimulus location that evoked excitation is outlined with a red box (dD5; *top left*). The horizontal black line below the *x*-axis (PSTH; *bottom left*) indicates the stimulus duration, which is also indicated by the gray shading on the PSTH and raster plots. All filled PSTHs in this and other figures are smoothed using a boxcar filter (filter width = 5, 1-ms bins). *E*: overlapping PSTHs indicate how the response patterns of unit 11a change when different hand locations are stimulated. PSTHs, in response to each of the single-site stimulation locations, are shown with colored lines corresponding to the specific stimulus location.

the significance test results from areas 3a and 3b combined to compare with values reported in the text.

Across cases, when we identified suppressive response occurrences of a given unit due to stimulation on a hand location, the majority of the responses to stimulation within the peak activation region included a transient excitatory response (E, 313/916, 34%) or transient excitatory response followed by a period of firing inhibition (E-I, 233/916, 25%). Almost 21% of neuronal responses (191/916) decreased the baseline firing rate in response to stimulation without a preceding excitatory response (I; Fig. 3). The remaining 19.5% (179/916) of neuronal responses did not deviate significantly from baseline firing during the tactile stimulation conditions delivered, classified as NS. Note that the E-I response type is similar to "replacing inhibition," reported by Hsiao and colleagues [e.g., Sripati et al. (2006)], whereas E and I are similar to traditional excitatory and inhibitory response types, respectively.

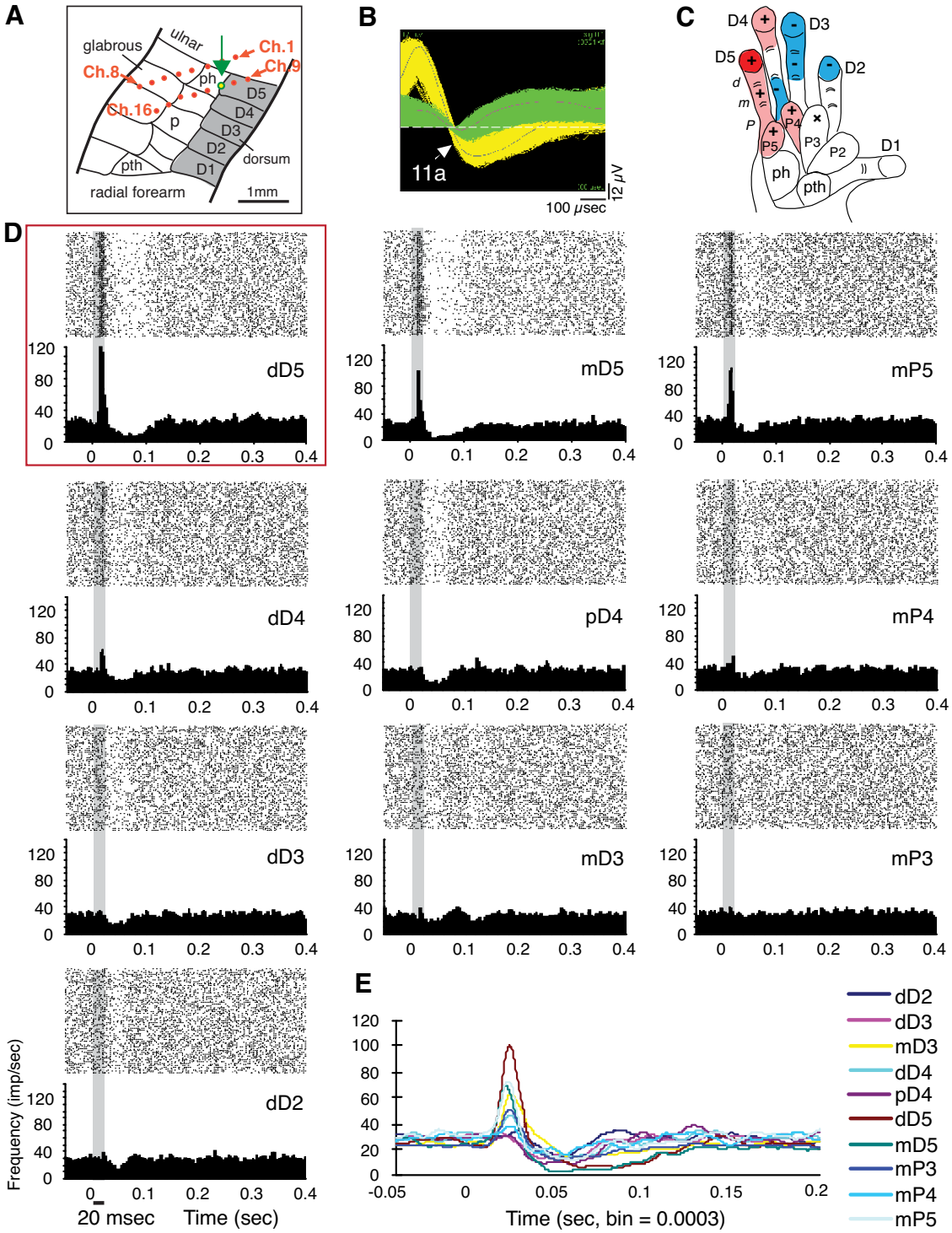

Table 2. *Results from area 3b compared with area 3a and statistical significance from samples of 3a and 3b combined*

Group	Measure or Subtype	Variables to Compare	Mean (SD) Area 3b	*n* Area 3b	Mean (SD) Area 3a	*n* Area 3a	Statistic Area 3b	*P* Area 3b	*P* Areas 3a + 3b
E-I	Suppression latency	SU	33 (12)	223	81 (30)	10	$Z = -2.95$	0.003*	0.002*
		MU	36 (13)	682	70 (28)	33			
E-I	Duration	SU	49 (32)	223	60 (28)	10	$Z = -3.38$	0.001*	3.3×10^{-12}*
		MU	43 (33)	682	28 (19)	33			
I	Suppression latency	SU	20 (14)	150	18 (15)	41	$Z = -5.64$	1.7×10^{-8}*	8.6×10^{-5}*
		MU	25 (12)	209	27 (18)	14			
I	Duration	SU	33 (24)	150	83 (66)	41	$Z = -0.57$	0.57	0.083
		MU	42 (38)	209	23 (14)	14			
SU	Suppression latency	E-I	33 (12)	223	81 (30)	10	$Z = -10.96$	6.2×10^{-28}*	8.2×10^{-35}*
		I	20 (14)	150	18 (15)	41			
SU	Duration	E-I	49 (32)	223	45 (28)	10	$Z = -5.46$	4.7×10^{-8}*	3.1×10^{-4}*
		I	33 (24)	150	83 (66)	41			
SU	Excitation latency	E	9 (15)	295	18 (2)	18	$Z = -0.71$	0.48	0.16
		E-I	13 (29)	223	19 (6)	10			
SU	Latency of excitation/suppression	E	18 (8)	294	18 (2)	18	$\chi^2 = 1.19$	0.55	0.47
		E-I	17 (7)	223	19 (6)	10			
		I	20 (14)	150	18 (15)	41			
SU	Excitation peak firing	E	64 (92)	294	24 (21)	18	$Z = -5.53$	3.2×10^{-8}*	6.3×10^{-9}*
		E-I	79 (74)	223	30 (18)	10			
SU	E-I and I	Latency	–	373	–	51	$\rho = 0.27$	1.4×10^{-7}*	3.2×10^{-4}*
		Duration	–	373	–	51			
SU	E-I and I	Latency	–	387	–	51	$\rho = 0.15$	0.003*	4.2×10^{-4}*
		Peak firing	–	387	–	51			
SU	E-I and I	Duration	–	373	–	51	$\rho = 0.25$	1.3×10^{-6}*	0.088
		Peak firing	–	387	–	51			
SU	E, E-I, and I	Latency	–	339	–	51	$\rho = -0.18$	0.001*	0.001*
		Background firing	–	757	–	51			
SU	E-I and I	Location	–	379	–	51	$\rho = -0.20$	6.0×10^{-4}*	0.001*
		Duration	–	379	–	51			
SU	E-I and I	Location	–	379	–	51	$\rho = -0.11$	0.034*	0.001*
		Latency	–	379	–	51			
SU	E	Occurrences	–	282	–	18	$\rho = -0.979$	4.3×10^{-6}*	1.8×10^{-7}*
		Location	–	282	–	18			
SU	E-I	Occurrences	–	220	–	10	$\rho = -0.937$	1.9×10^{-4}*	1.5×10^{-8}*
		Location	–	220	–	10			
SU	I	Occurrences	–	107	–	41	$\rho = -0.402$	0.284	0.381
		Location	–	107	–	41			
SU	NS	Occurrences	–	129	–	1	$\rho = -0.452$	0.222	0.203
		Location	–	129	–	1			
SU	Response types (E, E-I, I, and NS)	Occurrences < median	–	120	–	70	$\chi^2 = 46.49$	4.5×10^{-10}*	1.5×10^{-7}*
		Location	–	120	–	70			

Results from area 3b recordings in anesthetized primates summarized and compared with *P* values (*$P < 0.05$) reported in RESULTS (of areas 3a and 3b analyzed together). Data from area 3a in an unanesthetized galago are listed; statistics not calculated on this small subset. Mean and SD reported for pair-wise comparisons in units of milliseconds (latency, duration) or spikes/second (peak firing). Means are not reported for Spearman's ρ correlation analysis and the nonparametric median test. E-I, excitatory-inhibitory; I, inhibitory; E, excitatory; NS, no significant firing change.

For each response occurrence of SU and MU activity, we calculated firing rates, latencies, and duration of activity suppression, focusing on suppressive response components, as described below.

Analysis of suppression latencies and durations of neurons in areas 3b and 3a. To summarize quantitatively response properties related to firing-rate suppression in our sample, we measured minimal latency and suppressive duration from units in all five cases, comprising eight hemispheres, regardless of stimulation location relative to the peak activation location. To compare the differences between SUs and MUs and between neurons with significant postexcitatory inhibition (E-I) or inhibition only (I, without preceding excitation), we divided the whole population of responses into several subgroups and plotted the frequency histograms in Fig. 5. The distributions of inhibitory latencies and durations of MUs ($n = 941$) and SUs ($n = 424$) were similar and overlapping, but the averages differed slightly. The mean inhibition latency of E-I responses was significantly different between SUs ($n = 233$ responses) with 35 ms and MUs ($n = 718$ responses) with 38 ms inhibition latencies ($Z = -2.72$, $P = 0.007$). Average inhibition latencies of I responses were significantly different between SUs ($n = 191$ responses) with 19 ms and MUs ($n = 223$ responses) with 25 ms ($Z = -6.84$, $P = 7.9 \times 10^{-12}$). The mean inhibition durations for E-I responses were significantly different between SUs with 49 ms durations and MUs with 42 ms ($Z = -3.93$, $P = 8.57 \times 10^{-5}$, $n = 946$). For I responses, no significant difference was detected in average inhibition durations between SUs with 43 ms and MUs with 41 ms durations ($Z = -1.74$, $P = 0.083$, $n = 414$). For the distributions of inhibition, with or without preceding excitatory responses, we found that inhibition latencies were shorter for SU

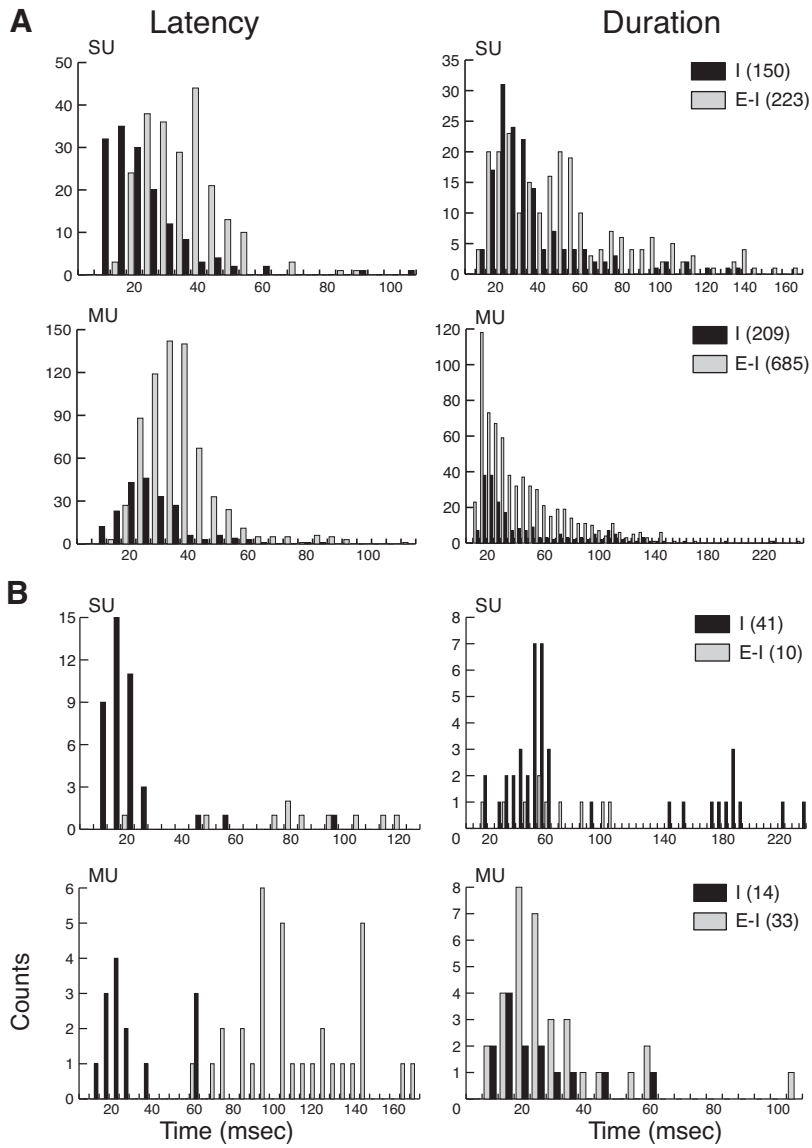

Fig. 5. Distributions of neuronal response latency (*left*) and suppressive response duration (*right*) for SU and multi-unit (MU) activity when ongoing baseline activity is suppressed (I; black bars) vs. when the suppression is preceded by increased firing (E-I; light gray bars). *A*: the majority of the sample consists of response occurrences from area 3b in anesthetized cases. *B*: response occurrences recorded in area 3a of an awake galago are shown separately. Counts on the *y*-axes and parentheses in the key indicate unit response occurrences. This latency measure is for the suppression component only, and thus the responses of suppression alone (I) tend to have earlier latencies than the E-I responses for both SU and MU activity. Histograms of the suppression durations appear relatively similar for SUs and MUs; however, note differences in the scales of the *x*- and *y*-axes.

responses than MU responses. The statistical differences may suggest that MU recordings include a somewhat different neuron population. However, MUs from many neurons firing at different excitatory (E) latencies may have caused firing suppression (I) to be detected at longer latencies. The E-I responses display, accordingly, significantly shorter response suppression durations for MUs than for SUs.

To evaluate relationships between inhibitory and excitatory response components further, we focused on the SU activity. As expected, the mean latency of the inhibitory component in the I response type (19 ms) was significantly shorter than when an excitatory component preceded the suppression in E-I (35 ms; $Z = -12.56$, $P = 3.63 \times 10^{-36}$, $n = 424$ neuronal responses). In our sample, the duration of the suppression was shorter for responses that showed suppression only (43 ms) compared with those that followed excitation (49 ms; $Z = -3.69$, $P = 2.19 \times 10^{-4}$, $n = 424$ neuronal responses). Thus for the responses in the E-I category, suppression occurred at longer latencies than suppression in the I category, suggesting that the excitatory response could have masked the earliest part of the inhibitory response. Similarly, the inhibitory component likely masked excitation in I responses but was not able to mask the excitatory component of the E-I responses. We did not detect a difference in latency between peak responses for E-I and E categories ($Z = -1.02$, $P = 0.306$). Notably, we evaluated the average latency of I responses (16.3 ms) compared with the excitatory latency of E responses (16.6 ms) and excitatory latency of E-I responses (15.6 ms) and found no significant differences [Kruskal-Wallis $\chi^2 = 1.493$, degrees of freedom (df) = 2, $P = 0.474$, $n = 698$ neuronal responses]. Thus the mean latencies for each category of our sample were similar, with an overall mean latency of 16.2 ms. We also found a weak but significant negative correlation between background firing rates and response latencies of all three response types (I, E-I, E). The results indicated that increased firing excitability decreased both the inhibitory and excitatory latencies or increased the detection of both types of responses (Spearman's $\rho = -0.182$, $P = 0.001$, $n = 343$ responses).

Whereas we focused on firing-rate suppression, we also compared the peak firing rates of SU responses categorized as E-I vs. E. The average magnitude of the excitatory component was larger for E-I responses (77.9 impulses/second, $n = 246$)

vs. E responses (58.3 impulses/second, $n = 310$; Mann-Whitney U-test $= 2.72 \times 10^4$, $P = 6.33 \times 10^{-9}$, total $n = 556$ responses). This suggests that the suppression component of an E-I response is part of in-field inhibition in the central RF, whereas E only occurs when stimulus is farther from the central mRF of the neuron.

We then analyzed the E-I responses and I responses to examine relationships between inhibitory and excitatory components using correlation and regression analyses. For all responses with suppression (E-I or I), suppression duration was very weakly correlated with the latency of the suppression (Spearman's $\rho = 0.118$, $P = 3.215 \times 10^{-4}$, $n = 425$ neuronal responses with suppression durations of 10 ms or more). For the subset of responses in which an excitatory response preceded the suppression (E-I), suppression latency was weakly correlated with excitatory response magnitude (Spearman's $\rho = 0.229$, $P = 4.23 \times 10^{-4}$, $n = 234$ neuronal responses with suppression durations of 10 ms or more). However, a relationship was not detected between excitatory peak magnitude with suppression duration (Spearman's $\rho = 0.088$, $P = 0.181$, $n = 234$ SU responses with suppression durations of 10 ms or more). Overall, we found weak correlations between excitatory and inhibitory response components, but other factors must contribute to the variation in the latency and duration of suppression components beyond the excitatory response magnitude.

Response types in relation to stimulus sites across digits vs. within digits. We next tested how a neuron's response type changed in relation to the position of the stimulus on the hand. If peak neural responses are obtained for a site on a given part of a digit, then it is conceivable that comparisons of a neuron's responses to a given stimulus site located on an adjacent digit would differ from when the stimulus site was outside of the peak response site but within the same digit. Thus we examined neuron responses relative to different stimulus locations (e.g., across digits vs. within digits) using a classification ranking that we set (Fig. 6). For this ranking, the stimulus site that evoked the highest firing rate ("peak activation site" or "hot spot") was identified and assigned a rank value of zero. Increasing values were assigned to the remaining stimulus sites on the hand in a given recording session. Next, we approximated the average distances between adjacent phalanges (which can vary for different digits) on the hand for each species (galago = 0.85 cm, owl monkey = 1.1 cm, squirrel monkey = 0.91 cm) to obtain a general value to relate to the separation between different locations on the primate hand. We used the average distance value (rounded up to 1 for visualization purposes) across and within digits and pads, and this value was summed for each step away from the peak activation site. This "uniform" ranking was based on indications that anatomical connections in primary somatosensory cortex are similarly dense within digits and across different digits (Liao et al. 2013; Negyessy et al. 2013) rather than faithfully representing anatomical distances in the actual hand. We tested a second classification scheme (not shown), in which we assigned a larger separation value or penalty when the stimulus was located on digits different than the one containing the hot spot compared with locations on the same digit as the hot spot. This "biased" ranking, which favors stimulus sites located on the same digit as the hot spot, mimics relationships of anatomical continuities on the hand or mimics potential for cortical connections to differ by location (Fang et al. 2002). We used correlations between the values assigned to each scheme with the measures of the response properties of excitatory and inhibitory firing (peak latency, peak excitatory firing rate, inhibitory latency, inhibitory duration) to examine how well the response properties correlated to the stimulus locations.

We found few differences in correlations between response property measures and each of the two classification-ranking schemes for stimulus location, with one exception. The peak E latency was significantly correlated with the uniform rank values, shown in Fig. 6, and was not significantly correlated with the biased rank values (Spearman's $\rho = 0.088$, $P = 0.014$; Spearman's $\rho = 0.066$, $P = 0.066$, respectively, $n = 777$). However, relationships, such as with peak firing rate, suppression duration, etc., were similarly correlated for the two ranking types, often with slightly higher (but still weak) correlations for the uniform ranking. Such correlations were found for suppression duration (Spearman's $\rho = -0.164$, $P = 0.001$; Spearman's $\rho = -0.156$, $P = 0.001$, respectively, $n = 413$) and suppression latency (Spearman's $\rho = -0.167$, $P = 0.001$; Spearman's $\rho = -0.141$, $P = 0.004$, respectively, $n = 410$). Overall, we found no evidence that the excitatory and inhibitory responses to tactile stimulation on the hand occurred with stronger magnitudes or were more often driven by sites within a digit rather than across different digits or palm pads. This suggests that the somatotopic organization of the cortical representation of the hand is the important factor compared with the separation between digits, which varies with hand positions and tasks. To reduce redundancy while exploring the spatial relationships of suppressive responses to hand stimulation, we therefore used only the uniform categorization of hand locations (Fig. 6) in subsequent analyses.

With the focus on the uniform ranking to relate the occurrences of E, E-I, or I responses to the stimulation of a given site that was not located at the peak activation region, we found a strong inverse relationship between the number of occurrences of E or E-I responses and the location value (Spearman's $\rho = -0.992$, $P = 1.75 \times 10^{-7}$, $n = 305$ responses; Spearman's $\rho = -0.996$, $P = 1.54 \times 10^{-8}$, $n = 236$ responses, respectively); however, we did not detect significant correlations between the assigned location values from the location-ranking values and the occurrences of I suppressive responses (Spearman's $\rho = -0.333$, $P = 0.381$, $n = 116$ responses) or the occurrences of stimulation producing no significant change in firing rate (NS; Spearman's $\rho = -0.469$, $P = 0.203$, $n = 129$ responses). The presence of strong negative correlations between E response components and stimulus locations indicates that E response components in our sample occur less frequently, as the stimulus site is more distant from the excitatory peak activation region. However, the lack of correlation between I response components and stimulus locations indicates that the I components may be more diffuse or may not be correlated with the location of the peak activation region.

We then examined the widespread nature of the I and E response components, using the uniform-ranking values to relate to the stimulus locations. For all response categories of E, E-I, and I vs. NS, fewer responses were collected when

the stimulus was located at or beyond a separation equivalent of four phalanges away from the site evoking the maximum recorded firing rate (Fig. 6*A*; *x*-axis value = 4). This finding was supported by the nonparametric median test, which showed that the value of four was the first for which neuron response counts were significantly below the median ($\chi^2 = 34.508$, df = 3, $P = 1.548 \times 10^{-7}$, $n = 244$ responses). For the E category, no such responses were collected when the stimulus was located beyond the equivalent of seven phalanges away from the peak activation site (Fig. 6; *x*-axis value = 7). The response types that we found when the stimulus was the farthest away from the site of peak activation were the E-I and I categories.

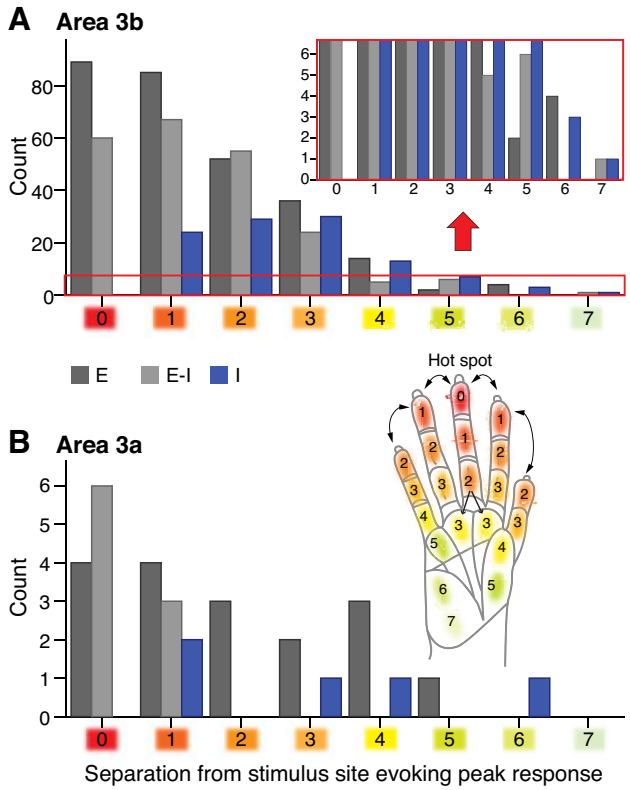

Fig. 6. Response type changes as the stimulus site is more separated from the site that evoked the highest firing rate for responses sampled from area 3b (*A*) and area 3a (*B*). Histogram of response types (E, dark gray; E-I, light gray; I, blue; see color key below *x*-axis in *A*) shows the distribution of value rankings (*x*-axis) related to the position of the tactile stimulation site compared with the stimulus site that evoked peak responses. For each recording experiment, a peak activation site, or hot spot (value = 0; red shading), was designated as the tactile stimulation location that evokes the highest neuronal peak responses among all of the stimulation sites during 1 experiment. We used a "uniform separation ranking" that sums the average distance between adjacent phalanges within digits (shown for squirrel monkey in the hand *inset* with values rounded up for visualization purposes) as the basis to assign a value relative to the hot spot for each (digit or palm) pad where the tactile stimulus was located during a recording session. Lighter shades are visual indicators of increasing values and increasing separation from the hot spot site, both on the hand schematic and on the *x*-axes. The red box in *A* indicates a portion of the histogram magnified above the red arrow, which is the same as the *y*-axis scale in *B* for response occurrences in area 3a. Response occurrences were fewer, but still detected, in units when the stimulation was several pads away from the peak activation location.

Profiles of Excitation and Inhibition Tracked across Multiple Stimulus Locations

When we examine the responses of SUs, we use the term "response profiles" to designate the set of response types (E, E-I, I, and NS) that we collected from that unit when different hand sites are stimulated during the same recording session (see example in Fig. 4). An individual neuron response decreases or increases and sometimes changes in type (e.g., from E-I to I or NS) as the stimulus is moved to different locations on the hand. For inclusion in this analysis, SUs should have responded to touch with an E, E-I, or I response type on at least one location on the hand. Response profiles were classified as "All E," "All I," "All E-I," or "Complex," depending on the set of response types presented by the unit when different locations in the hand were stimulated (see below). Across all five animals, we tracked 113 SU response profiles to hand stimulation. In four out of the five animals, we determined profiles when we held the same unit for recordings across five or more stimulus sites within 1 recording day. In one animal (OM-A), profiles were determined for sets of four or more sites, due to small sample sizes.

Profiles of excitation with inhibition. Most units responded to stimulation in different ways when we moved the probe to different hand sites. For >33% of the sample (38/113), the stimulation of a selected hand site resulted in initial excitatory responses, with or without subsequent inhibition, and then for the same unit, the stimulation of other hand sites resulted in firing-rate suppression. We termed this pattern a "complex response profile" type. Such profiles occurred in all species tested and in areas 3b and 3a (see Figs. 4, 7, and 8 to compare PG-B, PG-A, SM-A, respectively). We distinguished two subtypes of excitatory and inhibitory response profiles. For ~22% of our total sample (25/113), this inhibition for I and E-I responses occurred when the stimulus was immediately adjacent to the stimulus site that evoked the highest peak firing rate (peak activation site; Fig. 6, *x*-axis value = 1), either on the adjacent phalange within the same digit or on the matching phalange on an adjacent digit (Fig. 7). We use the term "adjacent-I" to indicate the suppression in response to stimulation on sites near the excitatory regions. In the remaining 13 profiles (nearly 12% of the total sample), neuron activity was suppressed only when the stimulus was more distant from the peak activation site (Fig. 6, *x*-axis value ≥ 2, and Figs. 4 and 8). We use the term "nonadjacent-I" to indicate suppression in response to stimulation on sites far from the site that evoked the highest peak firing.

In nearly 33% of the sample (37/113), stimulating selected hand sites resulted in initial excitatory responses, with or without subsequent inhibition, but excitation always preceded suppression (response profile type All E-I; Fig. 9). We termed this an All E-I response profile, and we categorized adjacent-I and nonadjacent-I subtypes of this pattern. Adjacent-I is in-field inhibition, in which suppression followed the initial excitatory response when the stimulus site was adjacent to the peak activation site. This occurred in ~19% of our total sample (22/113). In the remaining 15 profiles (>13% of the total sample), in-field inhibition only occurred when the stimulus was more distant from the peak activation site (nonadjacent-I).

Profiles of inhibition or excitation. For a small number of neuron units, none of the tested hand locations and stimulus

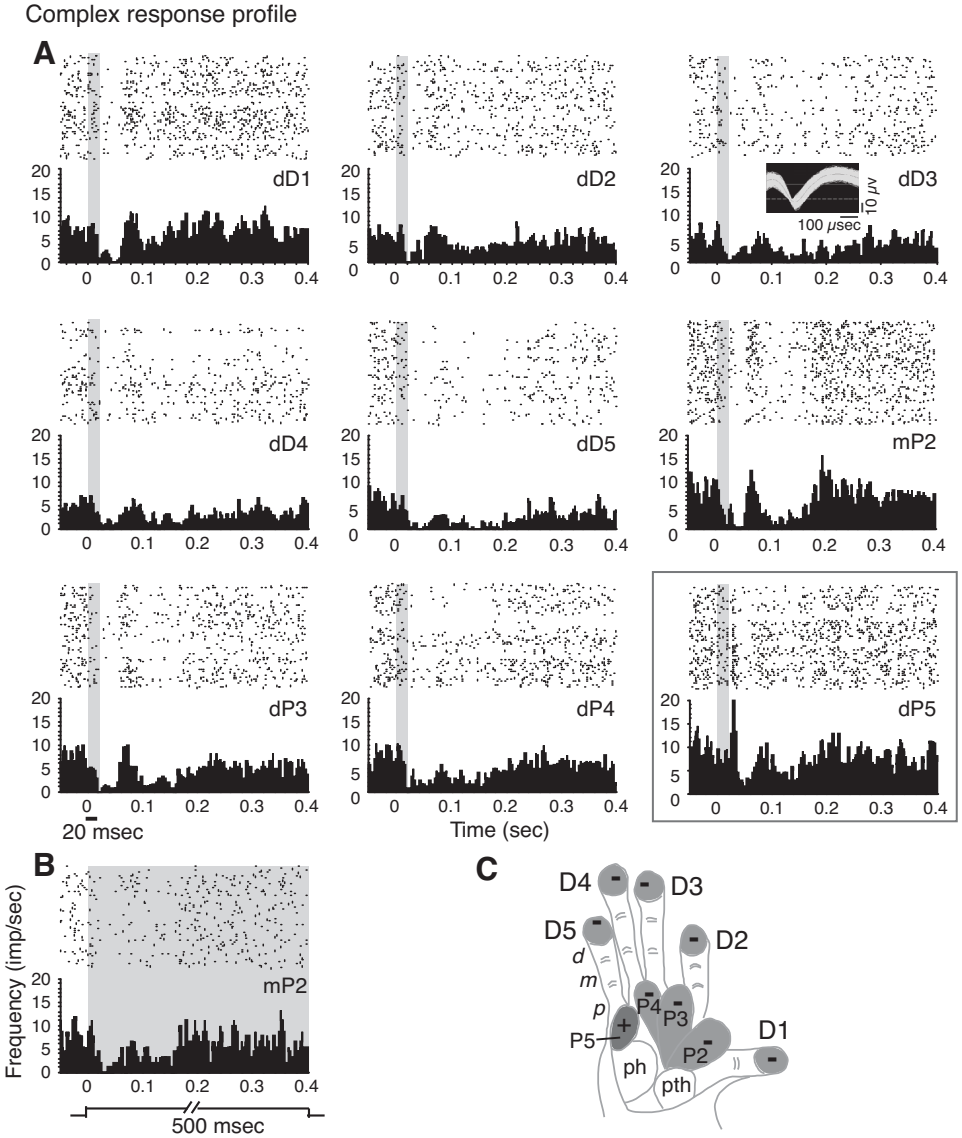

Fig. 7. Rasters and PSTHs from a recording session in galago PG-A track a typical complex response profile, characterized by excitatory and/or inhibitory responses, depending on the location of the stimulation site. Note that in this example, the electrode array was primarily located in area 3a, and PG-A was not anesthetized during the recording session. The horizontal black line below the *x*-axis (PSTH; *bottom left*) indicates the stimulus duration, which is also indicated by the gray shading on the PSTH and raster plots. *A*: PSTH and raster plots of unit activity (53a) are shown for several sites, and the site corresponding to the stimulus location that evoked peak excitation is outlined with a gray box. An image of the unit 53a waveforms recorded during single-site stimulation is shown the *inset* (*top right*). Most stimulations presented here indented the skin for 20 ms before leaving the skin at 1 cycle/second. In such conditions, suppression after skin indentation lasted from 20 to 40 ms before firing gradually recovered to baseline levels. *B*: PSTH and raster example shows that when the skin was indented for longer periods (500 ms), suppression duration was not maintained for the entire indentation period. *C*: the schematic of the galago hand indicates the responses of the neuron when different hand sites were stimulated. For visualization purposes, shaded regions indicate phalanges or palm pads on which the stimulus probe was placed. Light gray shading and the − symbols represent I responses. The + symbol represents E or E-I response, with the dark shade indicating the stimulus site that evoked the highest responses.

parameters evoked excitatory responses, even though these neurons were located in the hand representation in area 3b (21 SUs; 28 MUs) or area 3a (7 SUs; 1 MU for case PG-A). These neurons were detected by firing-rate suppression due to single-site skin indentation. The tactile response profiles for nearly 19% of our sample (21/113 response profiles) can be summarized as suppressed firing rates without an initial excitatory response to stimulation on all of the tested hand sites on the glabrous hand or did not evoke a significant increase from baseline firing rates. An example of such a response profile when all of the hand sites tested resulted in suppression or no significant response (All I profile) is shown in Fig. 10. For the remaining 15% of our sample (17/113), we found that stimulation at all tested hand sites significantly increased the neuronal firing rate over baseline firing in response to stimulation on all of the tested hand sites (All E profile). An example is shown in Fig. 11. For both the All E and All I response profile categories, it is possible that untested stimulation parameters would result in different response patterns, but this remains unknown.

Overall, the response profiles tracked from our recordings revealed E and I components of responses to single-site stimulation on the hand at different locations. The different response profiles found in our sample illustrate widespread unit responsiveness to stimulation delivered to individual sites located outside of the peak activation region (Fig. 12*A*). Counts of the different response profiles found in our sample revealed the predominance of response types that included both E and I components when sites beyond the peak activation location are stimulated (Fig. 12*B*). The variety of responses when stimulation occurs within and outside the peak activation location suggests that single-site stimulation evokes multiple suppression mechanisms that are likely important for stimulus representations in primary somatosensory cortex.

DISCUSSION

The goal of the present study was to report characteristics of the suppression of the ongoing baseline neuronal firing activity in somatosensory cortex of primates by tactile stimulation on a small (1 mm diameter) single site on the hand. Only a few

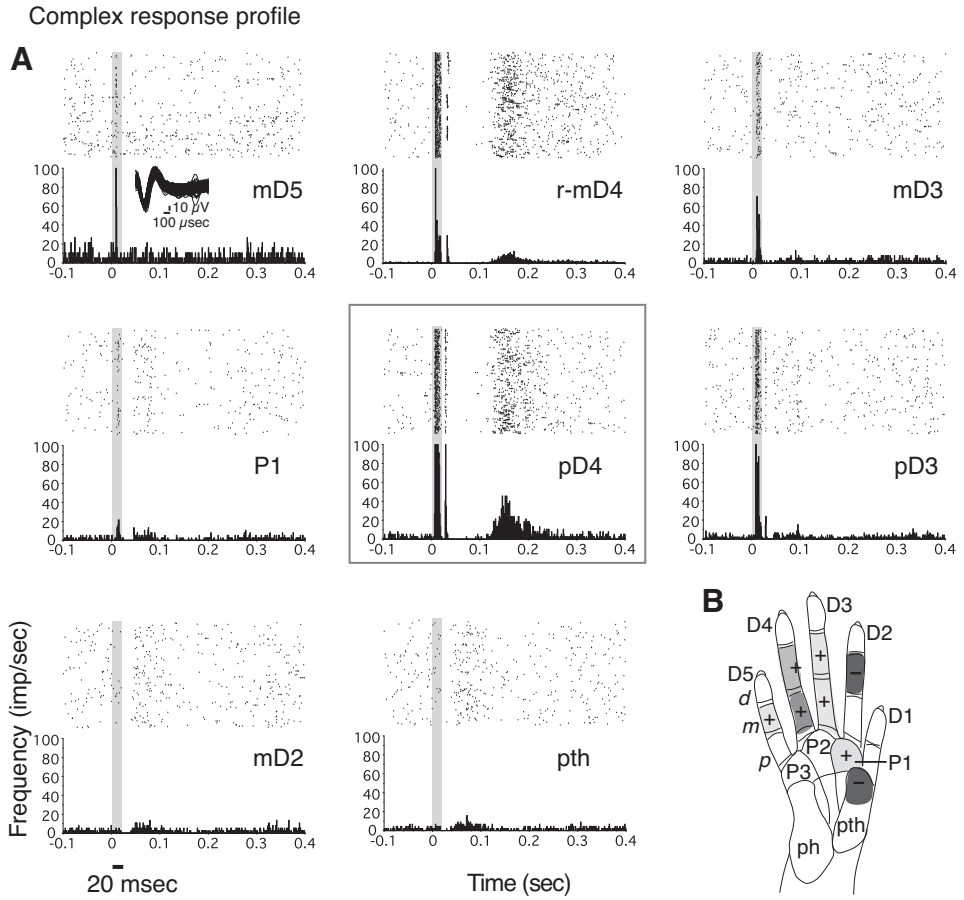

Fig. 8. *A*: example of a complex response profile of an SU (11a) from squirrel monkey SM-A to single-site stimulation on several hand sites within 1 recording session. Unit 11a waveforms recorded during single-site stimulation are shown in the *inset* (*top left*). r-mD4, radial mD4 (*top middle*). *B*: stimulation at locations beyond the hot spot (gray box around PSTH and raster for site pD4 and shading + symbols on hand schematic) resulted in weaker excitation (+ and lighter shadings on hand schematic, E-I and E response types). The stimulation of more distant sites on the hand from the hot spot suppressed firing without a preceding excitation (− and dark shading on hand schematic, I responses).

studies have described similar surround suppression of ongoing spontaneous activity, driven by single-site tactile stimulation in the somatosensory cortex of primates (Gardner and Costanzo 1980a, b), rodents (Sachdev et al. 2000; Swadlow 1989), and star-nosed moles (Sachdev and Catania 2002). In star-nosed moles, Sachdev and Catania (2002) reported that 40% of neurons that responded to single-site mechanosensory stimulation of the RF center were inhibited by stimulation of surrounding areas of skin on the same appendage on the star. In our study of the hand representation in monkeys, we showed that surround suppression can be found when stimulating single sites on separate digits and palm pads, at sites away from a given neuron's excitatory mRF on the hand. These results revealed spatially broad effects of the stimulus on the hand in the representation in primary somatosensory cortex in a new way. Our findings are consistent with those from studies using a "conditioning" stimulus preceding a "test" stimulus [e.g., Chowdhury and Rasmusson (2003); Gardner and Costanzo (1980a, b)], dual-probe stimuli (Lipton et al. 2010; Reed et al. 2010b), and complex multi-probe stimuli, pioneered by Johnson, Hsiao, and colleagues (DiCarlo et al. 1998; Fitzgerald et al. 2006a, b; Thakur et al. 2012). Similar findings have been reported for neurons in the visual system (Allman et al. 1985; Hubel and Wiesel 1962, 1965; Lee et al. 2013; Li et al. 2001) and the auditory system (Davis et al. 2003; Nelken and Young 1994; Shofner and Young 1985; Spirou and Young 1991).

Note that although we collected simultaneous neuronal recordings using chronically implanted electrode arrays, this report focuses on tracking individual neuronal responses when different hand sites are stimulated. Examinations of the relationships of multiple neurons or pairs of neurons are beyond the scope of this report, but others have reported on how stimulus location is represented within the somatosensory system in rodents and nonhuman primates (Ghazanfar et al. 2000; Nicolelis et al. 1998; Petersen and Diamond 2000). Due to the bias in our chronic recordings, the percentages reported here should not be considered to represent the population responses in primary somatosensory cortex, because we sampled a limited area (2 rows of 8 electrodes) over time. However, it is noteworthy that Sripati et al. (2006) characterized the RFs of distal digit pads in macaque monkeys using random patterns of tactile pulses, and they described similar categories. They noted 6% showed "excitation only," similar to type E; 42% with replacing inhibition, similar to type E-I; and 52% with "surround and replacing inhibition," which may resemble the complex response profile we find when stimulating sites across the hand rather than within a distal digit pad. Sripati et al. (2006) did not describe purely inhibitory fields, but those data were obtained from a single phalanx in awake macaques, constructed in response to pulses from a 400-probe tactile stimulator.

In the present experiments, such I suppression, without a conditioning stimulus, was detected in response to single-site stimuli (instead of dual- or multi-site stimuli) with chronically embedded electrodes for at least two reasons. First, the primates in our experiments were either awake (PG-A) or only lightly anesthetized or sedated to prevent hand movements. The detection of suppression depends on the level of ongoing

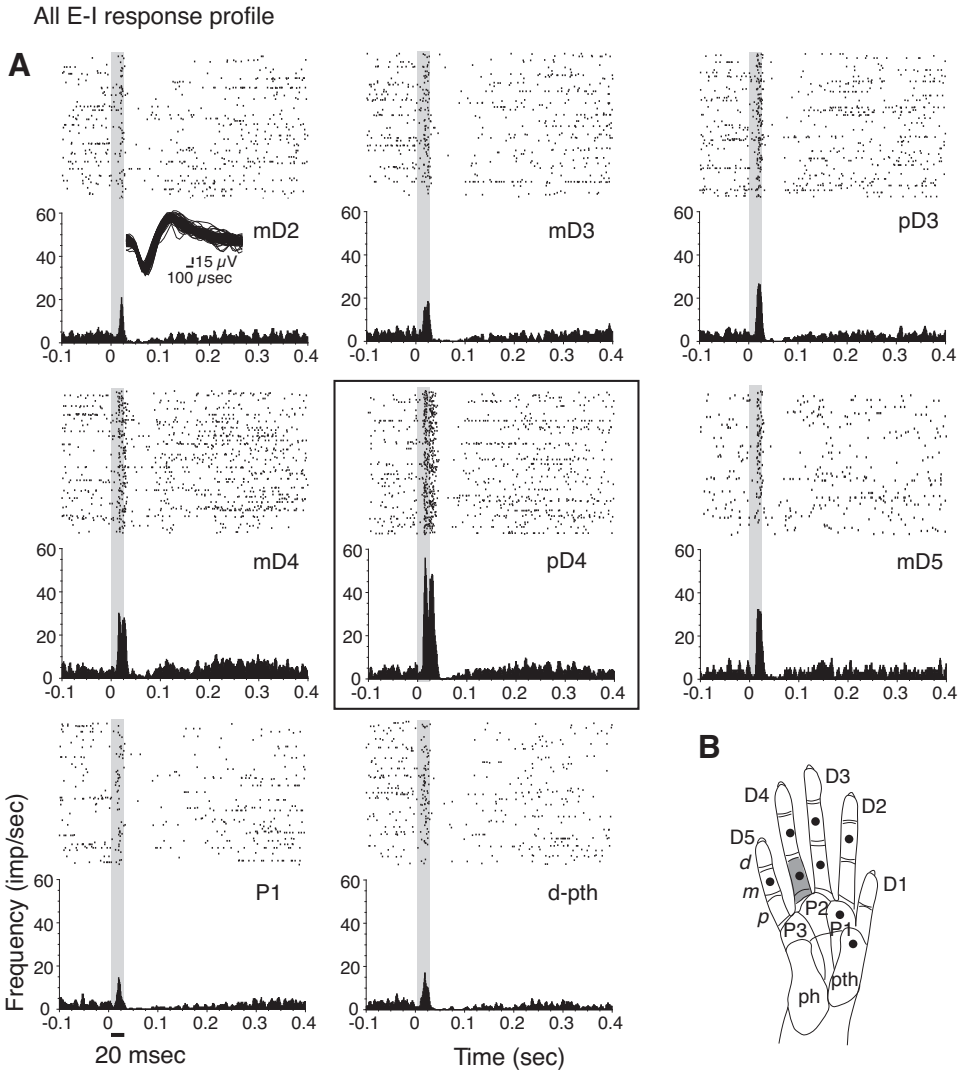

Fig. 9. *A*: example of excitatory responses followed by postexcitatory suppression to single-site stimulations on several hand sites within 1 recording session, making up an "All E-I" response profile for a unit (16a) from squirrel monkey SM-A. Waveforms of unit 16a, recorded during single-site stimulation, are shown in the *inset* (*top left*). *B*: gray shading on hand schematic indicates the hot spot in which tactile stimulation on pD4 evoked the highest firing rates (corresponding to the black box around the PSTH and raster in *A*) compared with the other sites tested in the recording session. Note that in contrast with the complex response profile (Figs. 7 and 8), this All E-I response profile does not include I responses alone for any of the tested stimulation sites. Filled circles in hand schematic mark stimulation locations.

activity that can be suppressed, and these experimental conditions resulted in baseline firing at higher levels than when recording neuronal activity under surgical anesthesia. Second, the microelectrode arrays allowed simultaneous collection of recording neuronal activity from multiple sites in the hand representation, and any given single stimulus location on the hand would fall within the mRF of some neurons and fall outside the mRF of most other recorded neurons. This avoided problems of focusing on individual neurons and the stimuli that increase their firing rates without investigating firing-rate suppression. Thus we use the mRF as a guide for stimulus placement and reference, but our report using suprathreshold stimulation results in neuron activations in response to stimuli that are beyond the mRF.

Properties and Extent of Widespread Responses and Suppressive Components

In the present experiments, stimulus responses characterized by excitation followed by inhibition had significantly higher magnitudes than responses that showed excitatory response components alone. Yet, the significant differences in firing-rate magnitudes did not translate into differences in excitation latencies between E and E-I types. The E-I response type we describe is similar to replacing inhibition described by Sripati et al. (2006), who suggest that the suppression component may not be simply refractoriness but may also reflect active cortical interactions. At the circuit level, the strongly activated neurons are also the neurons that are detectably inhibited. An activation threshold must be reached in a particular circuit to suppress a given neuron or circuit effectively. Thus we also found that weaker response facilitation tended to be related to weak or nonexistent firing suppression, consistent with traditional models of RF organization and balanced cortical circuits (Douglas et al. 1995; Sachdev et al. 2012; Wehr and Zador 2003). Additionally, when the ongoing firing was suppressed without preceding excitation, the latencies were not detectably different from our sample of excitation latencies. These relatively early latencies suggest the existence of short latency, direct subcortical activation of suppressive response components, as discussed for the visual system (Carandini et al. 2002) and somatosensory system [see Sachdev et al. (2012) review]. Notably, we recorded suppressive response types to touch in area 3a, similar to previous reports [e.g., Heath et al. (1976)], including initial inhibition of firing [e.g., Xu et al. (2011)]. Some inhibition latencies may be longer in our sample from area 3a (see Figs. 5 and 7), possibly reflecting

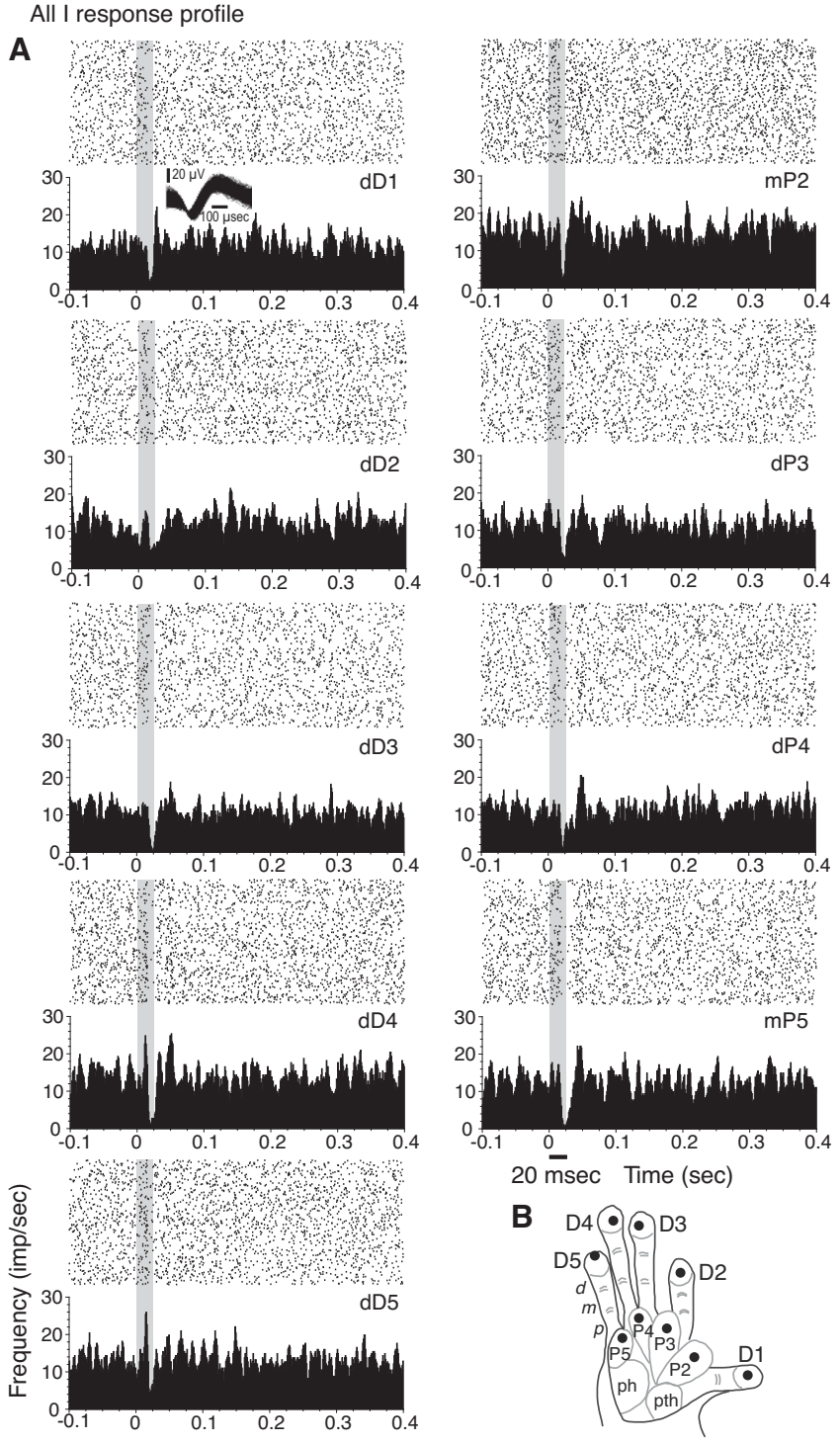

Fig. 10. Suppression in response to single-site stimulations within 1 recording session is shown in an example of an "All I" response profile for a unit (14b) from galago PG-B. *A*: rasters and PSTHs smoothed with a Gaussian filter show reduction of baseline activity in response to tactile stimulation at all tested locations on the hand (I response types), although the suppression for stimulation at dD2 is weak. The firing suppression peaked at 20–25 ms after stimulus onset. Waveforms of unit 14b are shown during single-site stimulation (*inset*, *top left*). *B*: the tested stimulation sites are shown on the galago hand schematic, with filled circles marking stimulation locations.

the route of tactile inputs from area 3b to 3a (Heath et al. 1976; Krubitzer and Kaas 1990; Wu and Kaas 2003). However, our sample from area 3a, in a case without sedation, is small, and we cannot interpret this data subset to generalize to area 3a across primates and across levels of sedation. Overall, we found neurons in areas 3b and 3a in different primate species and different levels of sedation that responded to skin indentations with suppression, particularly when the stimulated regions were distant from the site of peak excitatory firing.

We reported patterns of responses and response profiles that are widespread but not without limits. As the stimulus was presented at sites farther away from the peak activation site, the number of responses of any type that we collected for that unit decreased. We obtained I responses within one phalange or adjacent digit (1 step) but also farther away, and the response type collected at the farthest stimulus separation value was the I suppression (not including sites with no significant response). When comparing measured RF areas and overlap for measured cortical distances in area 3b of monkeys, Sur et al. (1980) used

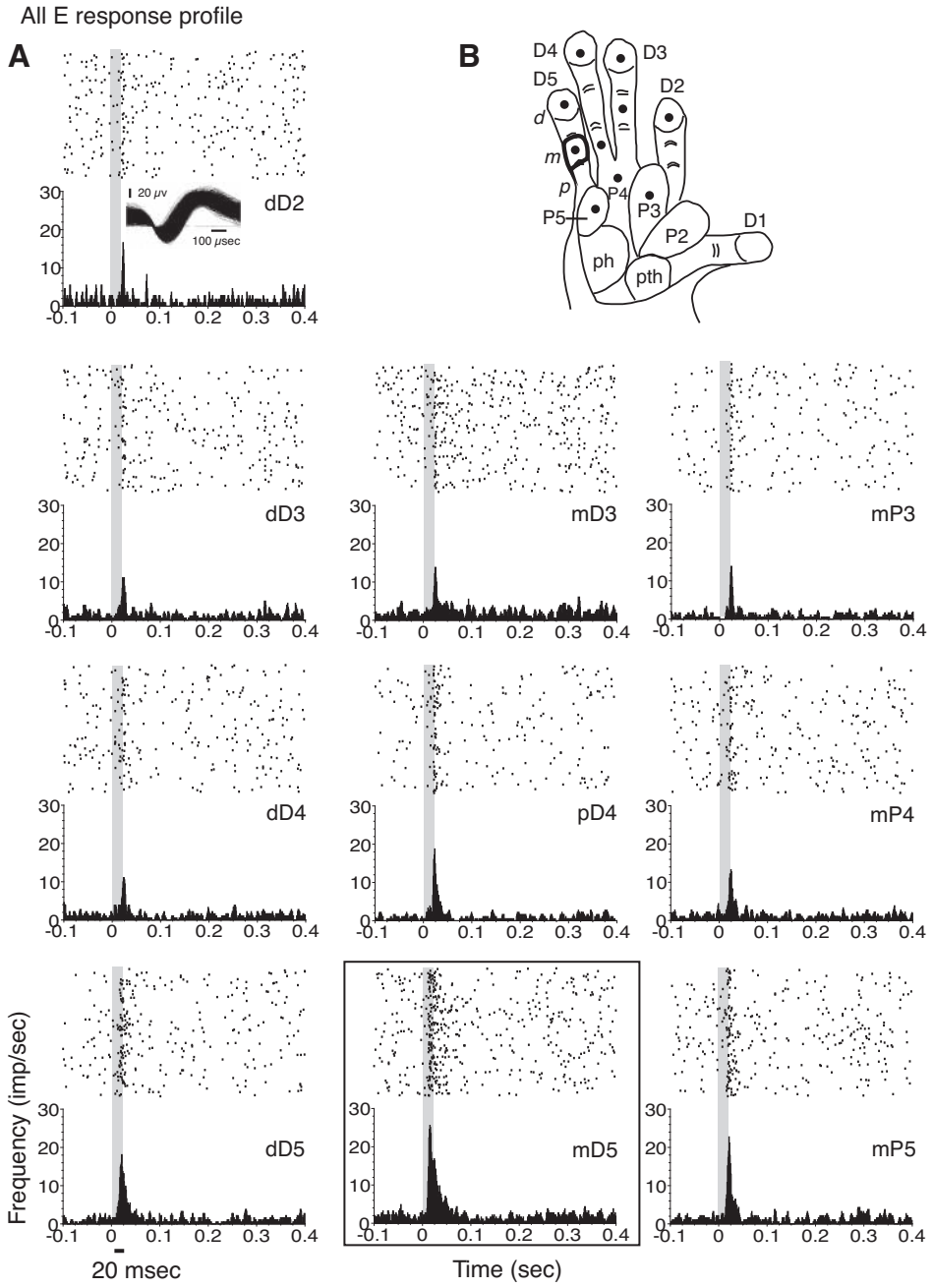

Fig. 11. Excitatory responses to all single-site stimulations within 1 recording session are depicted in an example of an "All E" response profile for a unit (10a) from galago PG-B. *A*: for this response profile type, units show E or E-I responses to tactile stimuli without any I responses. In contrast with the All E-I response profile, none of the tested locations resulted in NS. *B*: filled circles in the schematic of the galago hand show stimulation locations tested in the recording session. The outline in the hand diagram on mD5 corresponds to the site that evoked the highest responses, as shown in the PSTH indicated by the black box (*bottom middle*).

the concept of the hypercolumn for primary visual cortex from Hubel and Wiesel (1974). Sur et al. (1980) suggested that the primary somatosensory cortex hypercolumn would represent 1–1.5 mm diameter of cortex and that RFs are unlikely to overlap for neurons separated by a cortical distance of 500–600 μm in diameter. Whereas we did not calculate RF area or cortical distance, the multi-electrode arrays that we used here had an area of 0.4×2 mm^2 for two rows of eight microwires, $\sim$250 μm apart within each row. Our excitatory mRF mapping data for the five primate cases correspond to the example data by Sur et al. (1980) (Fig. 8), because the RFs tend to overlap slightly across neurons recorded from separate electrodes, 250 μm or more apart (see Fig. 1 for PG-B). Our observations of the suppressive I response types in relation to stimulus location may indicate a somewhat more extensive reach of suppression, as I responses were collected from individual neurons when the stimulus was distant from the site that evoked the highest peak firing in the given neuron. Additional studies are required to relate the locations on the hand that suppress a neuron's firing rates with the cortical distances between the territories corresponding to the representations of those hand locations.

In some ways, our findings resemble the long-range interactions in visual cortex, where stimuli that are outside the classical RF of neurons affect responses to stimuli within the RF [see Hallum and Movshon (2014) review], and short- and long-range cortical connections can contribute to the suppressive lateral interactions. However, here, we stimulated one location at a time and examined the response profiles of neurons, similar to reports by Moxon and colleagues (Tutunculer et al. 2006) using extracellular recordings in the rat

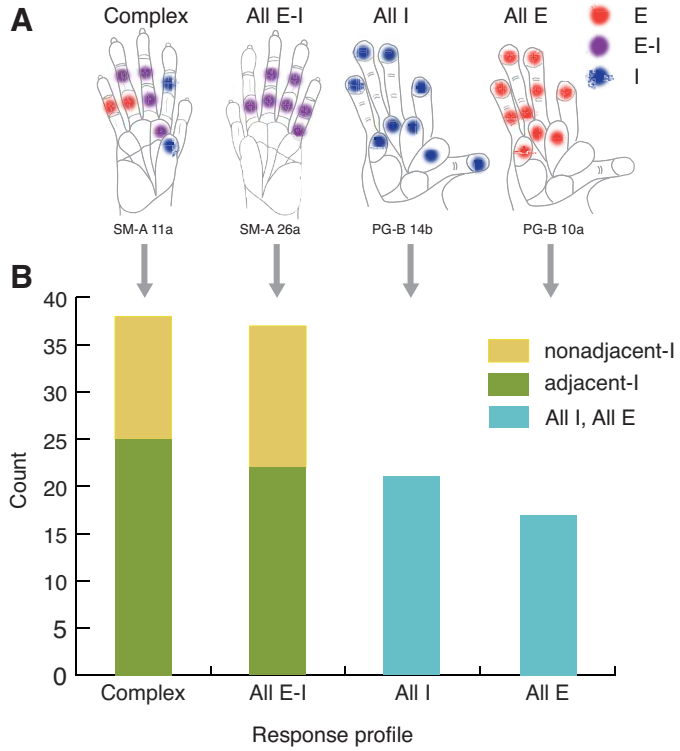

Fig. 12. Summary of response profile types (*A*) and tallies of response profiles (*B*) for SUs. *A*: response types for single-site stimulation are indicated by different colors: E only (red), E-I (violet), and I only (blue). Response profiles correspond to the summary of the response types obtained for all hand locations tested in a given recording session and can be classified as "Complex," All E-I, All I, or All E. Examples of each response profile were selected from actual cases for illustration. *B*: tallies of response types and subtypes are shown for the SU responses collected. "adjacent-I" indicates inhibition occurred when the stimulus was immediately adjacent to the stimulus site that evoked the highest peak firing rate (peak activation site) within a recording session for a given unit, either on the adjacent phalange within the same digit or on the matching phalange on an adjacent digit. "nonadjacent-I" indicates responses were suppressed only when the stimulus was more distant from the peak activation site or hot spot within a recording session.

forelimb representation of primary somatosensory cortex. We focused on characterizing suppressive response components in primary somatosensory cortex of nonhuman primates, in contrast to focusing on excitatory response fields. Yet, similar to results for excitatory RFs, we revealed effects of single-site stimulation that occurred far from each neuron's excitatory mRF across distant digits or palm pads. As reported by Tutunculer et al. (2006), we also found evidence to suggest that the response types to tactile stimuli were more closely related to cortical separations within the hand representation than to separations between contiguous surfaces of the physical hand. Furthermore, neuronal activity recorded from a selected cortical electrode in response to stimulation of sites across the hand suggested that lateral interactions involving firing suppression occur not only along the representation of a single digit (in the rostral-caudal dimension in cortex) but also between digits (across the medial-lateral dimension in cortex).

The response types and profiles reported here for the representation of the hand in primary somatosensory cortex are consistent with intracellular recording studies. Intracellular recordings reveal that the amplitude of excitatory postsynaptic potentials (EPSPs) and inhibitory postsynaptic potentials (IPSPs) varies with stimulus location, such that stimulating points at the center of the RF evoking the largest EPSP also evoke the largest IPSPs. Both EPSP and IPSP amplitudes decay with increasing separation from the RF center, with more gradual decay of IPSP strength (Andersson 1965; Gabernet et al. 2005; Innocenti and Manzoni 1972; Whitehorn and Towe 1968). This distribution is similar to the response profiles shown in studies with awake macaques (Gardner and Costanzo 1980a, b; Laskin and Spencer 1979) and response profiles in the present report.

Possible Significance of Widespread Suppressive Response Components

Overall, our results of I suppression properties, including the latencies that do not differ from initial E responses, are consistent with reports of subcortical sources of suppression in primary somatosensory cortex in rodents by Higley and Contreras (2007) and others [see Sachdev et al. (2012) review], as well as in other sensory systems and species (Bolz and Gilbert 1986; Carandini et al. 2002; Cavanaugh et al. 2002; Mickey and Middlebrooks 2005; Ojima and Murakami 2002). Yet, we also found evidence consistent with cortical sources of inhibition (Davis et al. 2003; Fitzpatrick et al. 1999; Hubel and Wiesel 1965; Nelken and Young 1994; Shofner and Young 1985; Spirou and Young 1991; Walker et al. 1999; Webb et al. 2005; Wehr and Zador 2003). Thus our findings indirectly support recent views that suppressive response components arise from a combination of cortical and subcortical sources rather than from the traditional model of suppression from cortical sources only [e.g., Sachdev et al. (2012) review].

Finally, we suggest that these results also support the idea that cortical reactivation and reorganization after sensory loss involve reductions of inhibition that span essentially the entire hand representation, which in turn, allows previously subthreshold activations to elicit neuronal firing (Jain et al. 2008; Oliveira et al. 2014; Qi et al. 2011, 2014). The extent of suppressive response components when single sites were stimulated across hand locations adds properties of firing suppression to the overall picture of RF structure and supports findings related to widespread excitatory response fields reported in the somatosensory cortex of primates (Friedman et al. 2008; Lipton et al. 2010; Reed et al. 2008, 2010a, b, 2011, 2012; Thakur et al. 2012; Tutunculer et al. 2006) and rodents (Tutunculer et al. 2006). We believe that our findings reported here contribute to a better understanding of how primates process sensory stimuli on the hand for object perception and manipulation, which is fundamental for developing strategies to improve sensorimotor functions of the hand after impairments in patients with deficits due to nerve or spinal cord injury and disorders.

ACKNOWLEDGMENTS

The authors thank Laura Trice for technical support and Dr. Troy Hackett for assisting array implantation surgeries. The authors appreciate this opportunity to contribute to this series in honor of Steven Hsiao, a wonderful scientist and a special friend to so many of us.

Present address of N. Jain: National Brain Research Centre, Manesar, India.

Present address of Y. Kajikawa: Cognitive Neuroscience and Schizophrenia Program, Nathan S. Kline Institute for Psychiatric Research, Orangeburg, New York 10962.

GRANTS

Support for this work was provided by the National Institute of Neurological Disorders and Stroke Grant NS16446 and James S. McDonnell Foundation (to J. H. Kaas); National Institute of Neurological Disorders and Stroke Grant NS067017 (to H.-X. Qi); National Institute of Neurological Disorders and Stroke Grant F31 NS053231 (to J. L. Reed); and Coordination for the Improvement of Higher Education Personnel (CAPES) grant (proc. 230/02-2; to J. G. Franca).

DISCLOSURES

No conflicts of interest, financial or otherwise, are declared.

AUTHOR CONTRIBUTIONS

Author contributions: H.-X.Q., J.L.R., J.G.F., N.J., Y.K., and J.H.K. conception and design of research; H.-X.Q., J.L.R., J.G.F., and N.J. performed experiments; H.-X.Q., J.L.R., and Y.K. analyzed data; H.-X.Q., J.L.R., and J.H.K. interpreted results of experiments; H.-X.Q. and J.L.R. prepared figures; H.-X.Q., J.L.R., Y.K., and J.H.K. drafted manuscript; H.-X.Q., J.L.R., J.G.F., N.J., Y.K., and J.H.K. edited and revised manuscript; H.-X.Q., J.L.R., J.G.F., N.J., Y.K., and J.H.K. approved final version of manuscript.

REFERENCES

Allman J, Miezin F, McGuinness E. Stimulus specific responses from beyond the classical receptive field: neurophysiological mechanisms for local-global comparisons in visual neurons. *Annu Rev Neurosci* 8: 407–430, 1985.

Alloway KD, Burton H. Differential effects of GABA and bicuculline on rapidly- and slowly-adapting neurons in primary somatosensory cortex of primates. *Exp Brain Res* 85: 598–610, 1991.

Andersson SA. Intracellular postsynaptic potentials in the somatosensory cortex of the cat. *Nature* 205: 297–298, 1965.

Arce-McShane FI, Hatsopoulos NG, Lee JC, Ross CF, Sessle BJ. Modulation dynamics in the orofacial sensorimotor cortex during motor skill acquisition. *J Neurosci* 34: 5985–5997, 2014.

Bolz J, Gilbert CD. Generation of end-inhibition in the visual cortex via interlaminar connections. *Nature* 320: 362–365, 1986.

Carandini M, Heeger DJ, Senn W. A synaptic explanation of suppression in visual cortex. *J Neurosci* 22: 10053–10065, 2002.

Carlson M, Welt C. Somatic sensory cortex (SmI) of the prosimian primate *Galago crassicaudatus*: organization of mechanoreceptive input from the hand in relation to cytoarchitecture. *J Comp Neurol* 189: 249–271, 1980.

Cavanaugh JR, Bair W, Movshon JA. Selectivity and spatial distribution of signals from the receptive field surround in macaque V1 neurons. *J Neurophysiol* 88: 2547–2556, 2002.

Chowdhury SA, Rasmusson DD. Corticocortical inhibition of peripheral inputs within primary somatosensory cortex: the role of GABA(A) and GABA(B) receptors. *J Neurophysiol* 90: 851–856, 2003.

Chubbuck JG. Small-motion biological stimulator. *Johns Hopkins APL Tech Digest* 5: 18–23, 1966.

Davis KA, Ramachandran R, May BJ. Auditory processing of spectral cues for sound localization in the inferior colliculus. *J Assoc Res Otolaryngol* 4: 148–163, 2003.

DiCarlo JJ, Johnson KO, Hsiao SS. Structure of receptive fields in area 3b of primary somatosensory cortex in the alert monkey. *J Neurosci* 18: 2626–2645, 1998.

Dickey AS, Suminski A, Amit Y, Hatsopoulos NG. Single-unit stability using chronically implanted multielectrode arrays. *J Neurophysiol* 102: 1331–1339, 2009.

Douglas RJ, Koch C, Mahowald M, Martin KA, Suarez HH. Recurrent excitation in neocortical circuits. *Science* 269: 981–985, 1995.

Dykes RW, Landry P, Metherate R, Hicks TP. Functional role of GABA in cat primary somatosensory cortex: shaping receptive fields of cortical neurons. *J Neurophysiol* 52: 1066–1093, 1984.

Fang PC, Jain N, Kaas JH. Few intrinsic connections cross the hand-face border of area 3b of New World monkeys. *J Comp Neurol* 454: 310–319, 2002.

Fitzgerald PJ, Lane JW, Thakur PH, Hsiao SS. Receptive field properties of the macaque second somatosensory cortex: representation of orientation on different finger pads. *J Neurosci* 26: 6473–6484, 2006a.

Fitzgerald PJ, Lane JW, Thakur PH, Hsiao SS. Receptive field (RF) properties of the macaque second somatosensory cortex: RF size, shape, and somatotopic organization. *J Neurosci* 26: 6485–6495, 2006b.

Fitzpatrick DC, Kuwada S, Kim DO, Parham K, Batra R. Responses of neurons to click-pairs as simulated echoes: auditory nerve to auditory cortex. *J Acoust Soc Am* 106: 3460–3472, 1999.

Friedman RM, Chen LM, Roe AW. Responses of areas 3b and 1 in anesthetized squirrel monkeys to single- and dual-site stimulation of the digits. *J Neurophysiol* 100: 3185–3196, 2008.

Gabernet L, Jadhav SP, Feldman DE, Carandini M, Scanziani M. Somatosensory integration controlled by dynamic thalamocortical feed-forward inhibition. *Neuron* 48: 315–327, 2005.

Gardner EP, Costanzo RM. Spatial integration of multiple-point stimuli in primary somatosensory cortical receptive fields of alert monkeys. *J Neurophysiol* 43: 420–443, 1980a.

Gardner EP, Costanzo RM. Temporal integration of multiple-point stimuli in primary somatosensory cortical receptive fields of alert monkeys. *J Neurophysiol* 43: 444–468, 1980b.

Ghazanfar AA, Stambaugh CR, Nicolelis MA. Encoding of tactile stimulus location by somatosensory thalamocortical ensembles. *J Neurosci* 20: 3761–3775, 2000.

Hallum LE, Movshon JA. Surround suppression supports second-order feature encoding by macaque V1 and V2 neurons. *Vision Res* 104: 24–35, 2014.

Heath CJ, Hore J, Phillips CG. Inputs from low threshold muscle and cutaneous afferents of hand and forearm to areas 3a and 3b of baboon's cerebral cortex. *J Physiol* 257: 199–227, 1976.

Higley MJ, Contreras D. Cellular mechanisms of suppressive interactions between somatosensory responses in vivo. *J Neurophysiol* 97: 647–658, 2007.

Hsiao S. Central mechanisms of tactile shape perception. *Curr Opin Neurobiol* 18: 418–424, 2008.

Hsiao SS, Bensmaia SJ. Coding of object shape and texture. In: *The Senses: A Comprehensive Reference*, edited by Gardner EP and Kaas JH. Waltham, MA: Elsevier, 2008, vol. 6, p. 55–66.

Hubel DH, Wiesel TN. Receptive fields and functional architecture in two nonstriate visual sreas (18 and 19) of the cat. *J Neurophysiol* 28: 229–289, 1965.

Hubel DH, Wiesel TN. Receptive fields, binocular interaction and functional architecture in the cat's visual cortex. *J Physiol* 160: 106–154, 1962.

Hubel DH, Wiesel TN. Uniformity of monkey striate cortex: a parallel relationship between field size, scatter, and magnification factor. *J Comp Neurol* 158: 295–305, 1974.

Huffman KJ, Krubitzer L. Area 3a: topographic organization and cortical connections in marmoset monkeys. *Cereb Cortex* 11: 849–867, 2001.

Innocenti GM, Manzoni T. Response patterns of somatosensory cortical neurones to peripheral stimuli. An intracellular study. *Arch Ital Biol* 110: 322–347, 1972.

Iwamura Y, Tanaka M, Sakamoto M, Hikosaka O. Functional subdivisions representing different finger regions in area-3 of the 1st somatosensory cortex of the conscious monkey. *Exp Brain Res* 51: 315–326, 1983.

Jain N, Qi HX, Collins CE, Kaas JH. Large-scale reorganization in the somatosensory cortex and thalamus after sensory loss in macaque monkeys. *J Neurosci* 28: 11042–11060, 2008.

Jain N, Qi HX, Kaas JH. Long-term chronic multichannel recordings from sensorimotor cortex and thalamus of primates. *Prog Brain Res* 130: 64–72, 2001.

Kim SS, Gomez-Ramirez M, Thakur PH, Hsiao SS. Multimodal interactions between proprioceptive and cutaneous signals in primary somatosensory cortex. *Neuron* 86: 555–566, 2015.

Krubitzer LA, Kaas JH. The organization and connections of somatosensory cortex in marmosets. *J Neurosci* 10: 952–974, 1990.

Laskin SE, Spencer WA. Cutaneous masking. II. Geometry of excitatory and inhibitory receptive fields of single units in somatosensory cortex of the cat. *J Neurophysiol* 42: 1061–1082, 1979.

Lee J, Kim K, Chung S, Lee C. Suppression of spontaneous activity before visual response in the primate V1 neurons during a visually guided saccade task. *J Neurosci* 33: 3760–3764, 2013.

Li W, Thier P, Wehrhahn C. Neuronal responses from beyond the classic receptive field in VI of alert monkeys. *Exp Brain Res* 139: 359–371, 2001.

Liao CC, Gharbawie OA, Qi H, Kaas JH. Cortical connections to single digit representations in area 3b of somatosensory cortex in squirrel monkeys and prosimian galagos. *J Comp Neurol* 521: 3768–3790, 2013.

Lipton ML, Liszewski MC, O'Connell MN, Mills A, Smiley JF, Branch CA, Isler JR, Schroeder CE. Interactions within the hand representation in primary somatosensory cortex of primates. *J Neurosci* 30: 15895–15903, 2010.

Merzenich MM, Kaas JH, Sur M, Lin CS. Double representation of the body surface within cytoarchitectonic areas 3b and 1 in "SI" in the owl monkey (*Aotus trivirgatus*). *J Comp Neurol* 181: 41–73, 1978.

Merzenich MM, Kaas JH, Wall J, Nelson RJ, Sur M, Felleman D. Topographic reorganization of somatosensory cortical areas 3b and 1 in adult monkeys following restricted deafferentation. *Neuroscience* 8: 33–55, 1983.

Mickey BJ, Middlebrooks JC. Sensitivity of auditory cortical neurons to the locations of leading and lagging sounds. *J Neurophysiol* 94: 979–989, 2005.

Mountcastle VB, Powell TP. Neural mechanisms subserving cutaneous sensibility, with special reference to the role of afferent inhibition in sensory perception and discrimination. *Bull Johns Hopkins Hosp* 105: 201–232, 1959.

Negyessy L, Palfi E, Ashaber M, Palmer C, Jakli B, Friedman RM, Chen LM, Roe AW. Intrinsic horizontal connections process global tactile features in the primary somatosensory cortex: neuroanatomical evidence. *J Comp Neurol* 521: 2798–2817, 2013.

Nelken I, Young ED. Two separate inhibitory mechanisms shape the responses of dorsal cochlear nucleus type IV units to narrowband and wideband stimuli. *J Neurophysiol* 71: 2446–2462, 1994.

Nelson RJ, Sur M, Felleman DJ, Kaas JH. Representations of the body surface in postcentral parietal cortex of *Macaca fascicularis*. *J Comp Neurol* 192: 611–643, 1980.

Nicolelis MA, Chapin JK. Spatiotemporal structure of somatosensory responses of many-neuron ensembles in the rat ventral posterior medial nucleus of the thalamus. *J Neurosci* 14: 3511–3532, 1994.

Nicolelis MA, Dimitrov D, Carmena JM, Crist R, Lehew G, Kralik JD, Wise SP. Chronic, multisite, multielectrode recordings in macaque monkeys. *Proc Natl Acad Sci USA* 100: 11041–11046, 2003.

Nicolelis MA, Ghazanfar AA, Faggin BM, Votaw S, Oliveira LM. Reconstructing the engram: simultaneous, multisite, many single neuron recordings. *Neuron* 18: 529–537, 1997.

Nicolelis MA, Ghazanfar AA, Stambaugh CR, Oliveira LM, Laubach M, Chapin JK, Nelson RJ, Kaas JH. Simultaneous encoding of tactile information by three primate cortical areas. *Nat Neurosci* 1: 621–630, 1998.

Ojima H, Murakami K. Intracellular characterization of suppressive responses in supragranular pyramidal neurons of cat primary auditory cortex in vivo. *Cereb Cortex* 12: 1079–1091, 2002.

Oliveira JT, Bittencourt-Navarrete RE, de Almeida FM, Tonda-Turo C, Martinez AM, Franca JG. Enhancement of median nerve regeneration by mesenchymal stem cells engraftment in an absorbable conduit: improvement of peripheral nerve morphology with enlargement of somatosensory cortical representation. *Front Neuroanat* 8: 111, 2014.

Petersen RS, Diamond ME. Spatial-temporal distribution of whisker-evoked activity in rat somatosensory cortex and the coding of stimulus location. *J Neurosci* 20: 6135–6143, 2000.

Qi HX, Chen LM, Kaas JH. Reorganization of somatosensory cortical areas 3b and 1 after unilateral section of dorsal columns of the spinal cord in squirrel monkeys. *J Neurosci* 31: 13662–13675, 2011.

Qi HX, Reed JL, Gharbawie OA, Burish MJ, Kaas JH. Cortical neuron response properties are related to lesion extent and behavioral recovery after sensory loss from spinal cord injury in monkeys. *J Neurosci* 34: 4345–4363, 2014.

Reed JL, Pouget P, Qi HX, Zhou Z, Bernard MR, Burish MJ, Haitas J, Bonds AB, Kaas JH. Widespread spatial integration in primary somatosensory cortex. *Proc Natl Acad Sci USA* 105: 10233–10237, 2008.

Reed JL, Pouget P, Qi HX, Zhou Z, Bernard MR, Burish MJ, Kaas JH. Effects of spatiotemporal stimulus properties on spike timing correlations in owl monkey primary somatosensory cortex. *J Neurophysiol* 108: 3353–3369, 2012.

Reed JL, Qi HX, Kaas JH. Spatiotemporal properties of neuron response suppression in owl monkey primary somatosensory cortex when stimuli are presented to both hands. *J Neurosci* 31: 3589–3601, 2011.

Reed JL, Qi HX, Pouget P, Burish MJ, Bonds AB, Kaas JH. Modular processing in the hand representation of primate primary somatosensory cortex coexists with widespread activation. *J Neurophysiol* 104: 3136–3145, 2010a.

Reed JL, Qi HX, Zhou Z, Bernard MR, Burish MJ, Bonds AB, Kaas JH. Response properties of neurons in primary somatosensory cortex of owl monkeys reflect widespread spatiotemporal integration. *J Neurophysiol* 103: 2139–2157, 2010b.

Saal HP, Bensmaia SJ. Touch is a team effort: interplay of submodalities in cutaneous sensibility. *Trends Neurosci* 37: 689–697, 2014.

Sachdev RN, Catania KC. Receptive fields and response properties of neurons in the star-nosed mole's somatosensory fovea. *J Neurophysiol* 87: 2602–2611, 2002.

Sachdev RN, Krause MR, Mazer JA. Surround suppression and sparse coding in visual and barrel cortices. *Front Neural Circuits* 6: 43, 2012.

Sachdev RN, Sellien H, Ebner FF. Direct inhibition evoked by whisker stimulation in somatic sensory (SI) barrel field cortex of the awake rat. *J Neurophysiol* 84: 1497–1504, 2000.

Shofner WP, Young ED. Excitatory/inhibitory response types in the cochlear nucleus: relationships to discharge patterns and responses to electrical stimulation of the auditory nerve. *J Neurophysiol* 54: 917–939, 1985.

Spirou GA, Young ED. Organization of dorsal cochlear nucleus type IV unit response maps and their relationship to activation by bandlimited noise. *J Neurophysiol* 66: 1750–1768, 1991.

Sripati AP, Yoshioka T, Denchev P, Hsiao SS, Johnson KO. Spatiotemporal receptive fields of peripheral afferents and cortical area 3b and 1 neurons in the primate somatosensory system. *J Neurosci* 26: 2101–2114, 2006.

Sur M. Receptive fields of neurons in areas 3b and 1 of somatosensory cortex in monkeys. *Brain Res* 198: 465–471, 1980.

Sur M, Merzenich MM, Kaas JH. Magnification, receptive-field area, and "hypercolumn" size in areas 3b and 1 of somatosensory cortex in owl monkeys. *J Neurophysiol* 44: 295–311, 1980.

Sur M, Nelson RJ, Kaas JH. Representations of the body surface in cortical areas 3b and 1 of squirrel monkeys: comparisons with other primates. *J Comp Neurol* 211: 177–192, 1982.

Sur M, Wall JT, Kaas JH. Modular distribution of neurons with slowly adapting and rapidly adapting responses in area 3b of somatosensory cortex in monkeys. *J Neurophysiol* 51: 724–744, 1984.

Swadlow HA. Efferent neurons and suspected interneurons in S-1 vibrissa cortex of the awake rabbit: receptive fields and axonal properties. *J Neurophysiol* 62: 288–308, 1989.

Thakur PH, Fitzgerald PJ, Hsiao SS. Second-order receptive fields reveal multidigit interactions in area 3b of the macaque monkey. *J Neurophysiol* 108: 243–262, 2012.

Thakur PH, Fitzgerald PJ, Lane JW, Hsiao SS. Receptive field properties of the macaque second somatosensory cortex: nonlinear mechanisms underlying the representation of orientation within a finger pad. *J Neurosci* 26: 13567–13575, 2006.

Tutunculer B, Foffani G, Himes BT, Moxon KA. Structure of the excitatory receptive fields of infragranular forelimb neurons in the rat primary somatosensory cortex responding to touch. *Cereb Cortex* 16: 791–810, 2006.

Walker GA, Ohzawa I, Freeman RD. Asymmetric suppression outside the classical receptive field of the visual cortex. *J Neurosci* 19: 10536–10553, 1999.

Webb BS, Dhruv NT, Solomon SG, Tailby C, Lennie P. Early and late mechanisms of surround suppression in striate cortex of macaque. *J Neurosci* 25: 11666–11675, 2005.

Wehr M, Zador AM. Balanced inhibition underlies tuning and sharpens spike timing in auditory cortex. *Nature* 426: 442–446, 2003.

Whitehorn D, Towe AL. Postsynaptic potential patterns evoked upon cells in sensorimotor cortex of cat by stimulation at the periphery. *Exp Neurol* 22: 222–224, 1968.

Wong-Riley M. Changes in the visual system of monocularly sutured or enucleated cats demonstrable with cytochrome oxidase histochemistry. *Brain Res* 171: 11–28, 1979.

Wu CW, Kaas JH. Somatosensory cortex of prosimian galagos: physiological recording, cytoarchitecture, and corticocortical connections of anterior parietal cortex and cortex of the lateral sulcus. *J Comp Neurol* 457: 263–292, 2003.

Xu Y, Wang X, Peck C, Goldberg ME. The time course of the tonic oculomotor proprioceptive signal in area 3a of somatosensory cortex. *J Neurophysiol* 106: 71–77, 2011.